# Differences in berry primary and secondary metabolisms identified by transcriptomic and metabolic profiling of two table grape color somatic variants

Claudia Santibáñez[1,2,3], Carlos Meyer[1], Litsy Martínez[1], Tomás Moyano[4], John Lunn[5], Regina Feil[5], Zhanwu Dai[2], David Carrasco[6], Rosa Arroyo-García[6], Ghislaine Hilbert[2], Christel Renaud[2], Serge Delrot[2], Fabiane Manke-Nachtigall[3], Rodrigo Gutiérrez[4], José Tomás Matus[7]*, Eric Gomès[2]*, Patricio Arce-Johnson[1]*

[1] Laboratorio de Biología Molecular y Biotecnología Vegetal, Departamento de Genética Molecular y Microbiología, Facultad de Ciencias Biológicas, Pontificia Universidad Católica de Chile, Santiago 8331150, Chile.

[2] Université de Bordeaux, ISVV, INRA, UMR 1287 Ecophysiology and Functional Genomic of Grapevine, Villenave d'Ornon, France.

[3] Facultad de Ciencias de la Salud, Universidad Autónoma de Chile.

[4] FONDAP Center for Genome Regulation, Millennium Nucleus Center for Plant Systems and Synthetic Biology, Departamento de Genética Molecular y Microbiología, Facultad de Ciencias Biológicas, Ponticia Universidad Católica de Chile, Santiago 8331150, Chile

[5] Max Plant Institute of Molecular Plant Physiology, Wissenschaftspark Golm, Am Mühlenberg 1, 14476 Potsdam (OT) Golm, Germany.

[6] Centre for Plant Biotechnology and Genomics (UPM-INIA, CBGP), 28223 Pozuelo de Alarcón, Madrid. Spain.

[7] Institute for Integrative Systems Biology, I$^2$SysBio (Universitat de València - CSIC) 46980, Paterna, Spain.

*Correspondence: tomas.matus@uv.es; eric.gomes@inra.fr , parce@bio.puc.cl

## ABSTRACT

Anthocyanins are flavonoids responsible for the color of berries in skin-pigmented grapevine (*Vitis vinifera* L.). Due to the widely adopted vegetative propagation of this species, somatic mutations occurring in meristematic cell layers can be fixed and passed into the rest of the plant when cloned. In this study we focused on the transcriptomic and metabolic differences between two color somatic variants. Using microscopic, metabolic and mRNA profiling analyses we compared the table grape cultivar (cv.) 'Red Globe' (RG, with purplish berry skin) and cv. 'Chimenti Globe' (CG, with a contrasting reddish berry skin color). As expected, significant differences were found in the composition of flavonoids and other phenylpropanoids, but also in their upstream precursors' shikimate and phenylalanine. Among primary metabolites, sugar phosphates related with sucrose biosynthesis were less accumulated in cv. 'CG'. The red-skinned cv. 'CG' only contained di-hydroxylated anthocyanins (i.e. peonidin and cyanidin) while the tri-hydroxylated derivatives malvidin, delphinidin and petunidin were absent, in correlation to the reddish cv. 'CG' skin coloration. Transcriptomic analysis showed alteration in flavonoid metabolism and terpenoid pathways and in primary metabolism such as sugar content. Eleven *flavonoid 3'5'-hydroxylase* gene copies were down-regulated in cv. 'CG'. This family of cytochrome P450 oxidoreductases are key in the biosynthesis of tri-hydroxylated anthocyanins. Many transcription factors appeared down-regulated in cv. 'CG' in correlation to the metabolic and transcriptomic changes observed. The use of molecular markers and its confirmation with our RNA-seq data showed the exclusive presence of the null *MYBA2* white allele (i.e. homozygous in both L1 and L2 layers) in the two somatic variants. Therefore, the differences in *MYBA1* expression seem sufficient for the skin pigmentation differences and the changes in MYBA target gene expression in cv. 'Chimenti Globe'.

## INTRODUCTION

Table grapes are produced for their fresh and dried (i.e. raisins) consumption, with their markets continuously demanding better fruit quality but also searching for the generation of new cultivars with appealing features. The berry developmental process displays a double sigmoid curve with two growth phases separated by a lag phase, at the end of which veraison takes place (COOMBE, 1995). The accumulation of pigments (i.e. secondary metabolites known as anthocyanins) occurs at this stage in red and black-skinned cultivars, concomitant with sugars (primary metabolites) and other secondary metabolites (e.g. aroma volatile compounds). All these accumulate until the fruit exhibits its desirable quality traits and it is ready for harvest.

Berry skin color is an important trait for the grapevine industry, used as a criterion for selection within breeding programs. Berry skin colors ranges from black to blue, red or pink and also yellowish-green tones and hues, as a consequence of natural hybridization and human selection processes (Azuma, 2018; Azuma et al., 2008; Frédérique Pelsy, Dumas, Bévilacqua, Hocquigny, & Merdinoglu, 2015). Clonal polymorphism affecting berry color is a common event that occurs in grapevines thanks to vegetative propagation. Under these circumstances somatic mutations that occur in the meristematic cells within buds (in the entire meristem -bud sports- or only a portion -chimeras-) are maintained and propagated, leading to somatic color variants (Pelsy et al., 2015; D'Amato, 1997). In most cases, somatic mutations affect only one cell layer of the meristem, leading to periclinal chimeras. This phenomenon engenders a heritable variation source creating new grape cultivars.

The main somatic polymorphisms accounting for color variation include insertions, duplications or SNPs, some caused by the activity of transposable elements disturbing regulatory regions (Carrier et al., 2012). Some well-known examples of clonal polymorphism affecting berry color correspond to the case of cultivars (cv.) 'Pinot Noir' and 'Pinot Blanc', with the later presenting a large deletion (over 260 kb-long) that removes the functional *MYBA1* and *MYBA2* genes that are the main regulators of anthocyanin synthesis (Walker et al., 2006; Yakushiji et al., 2006). A different somatic mutation was found in cv. 'Pinot Gris' but which affected the same two genes, producing a grey-skinned phenotype. In this second variant a chimeric structure was identified, with berries composed of a colored L1-derived epidermis (heterozygous for the functional and null alleles) while the L2 cells possessed a homozygous mutation in both *MYBA1* and *MYBA2* (Vezzulli et al., 2012).

The *MYBA1* and *MYBA2* genes form part of the berry color locus found in chromosome 2 (Hocquigny et al., 2004). These factors are known to form ternary complexes with bHLH (basic helix–loop–helix) and WDR (tryptophan–aspartic acid repeat) proteins (Hichri et al., 2010; Matus et al., 2010) being all of them important for the activation of the structural genes of the flavonoid branch in the phenylpropanoid pathway. Additional factors have been identified to date in this species (Matus et al., 2017), demonstrating a complex hierarchical regulation of pigment accumulation according to organ and in response to the environment.

In the last decade several genome-wide studies have demonstrated that a large transcriptomic shift drives the transition from the green berry to the ripening stages (Fasoli et al., 2012; Massonnet et al., 2017; Palumbo et al., 2014). The availability of a high quality grapevine genomic sequence and of large amount of transcriptomics and metabolomics data has allowed to conduct integrative analyses to decipher the key transcriptomic reprogramming events occurring at the onset and very late stages of berry ripening (reviewed by (Serrano et al., 2017; Wong & Matus, 2017). However, most of the transcriptomic comparisons conducted so far have considered very distant cultivars (Ghan et al., 2015; Massonnet et al., 2017; Zenoni et al., 2016) while very few have compared closely related cultivars at the genome-wide level (Carbonell-Bejerano et al., 2017). Here, we performed a microscopic, metabolic and transcriptomic characterization of berry development and ripening in two almost isogenic cultivars with different berry skin pigmentation. Berries from the cultivar 'Red Globe' (RG), characterized by a large size, thick skin and dark purple skin color, were compared to those of its somatic variant cv. 'Chimenti Globe' (CG) with similar characteristics but differing in its skin color. The phenotype of 'CG' was initially observed in Talagante (Metropolitan Region, Chile) during grape harvest in 2005, within a cv. 'RG' field. 'Chimenti Globe' has reddish grape clusters and was selected by its producer for propagation via cuttings (www.chgchile.cl).

## MATERIALS AND METHODS

### Plant material and experimental design

Plant material used in this study corresponds to six plants of commercial table grape cv. 'Red Globe' (RG) and six plants of cv. 'Chimenti Globe' (CG), positioned in Camino Loreto,

Parcela 8-9, Talagante, (Región Metropolitana, Santiago of Chile; 33°38′26″S; 70°51′52″ W) (FIGURE 1A). Sampling was performed during seasons 2013 and 2014. Veraison stage was set as the period at which clusters were 30–50% colored and 5º Brix (5% w/w soluble solids) (FIGURE 1B), and the late ripening stage when berry sugar content reached 22-23°Brix (FIGURE 1C). One cluster from each plant (experimental unit) was randomly sampled in both cultivars, in the two stages and seasons. Berries were peeled, and berry skins were frozen in liquid nitrogen and stored at –80°C until required.

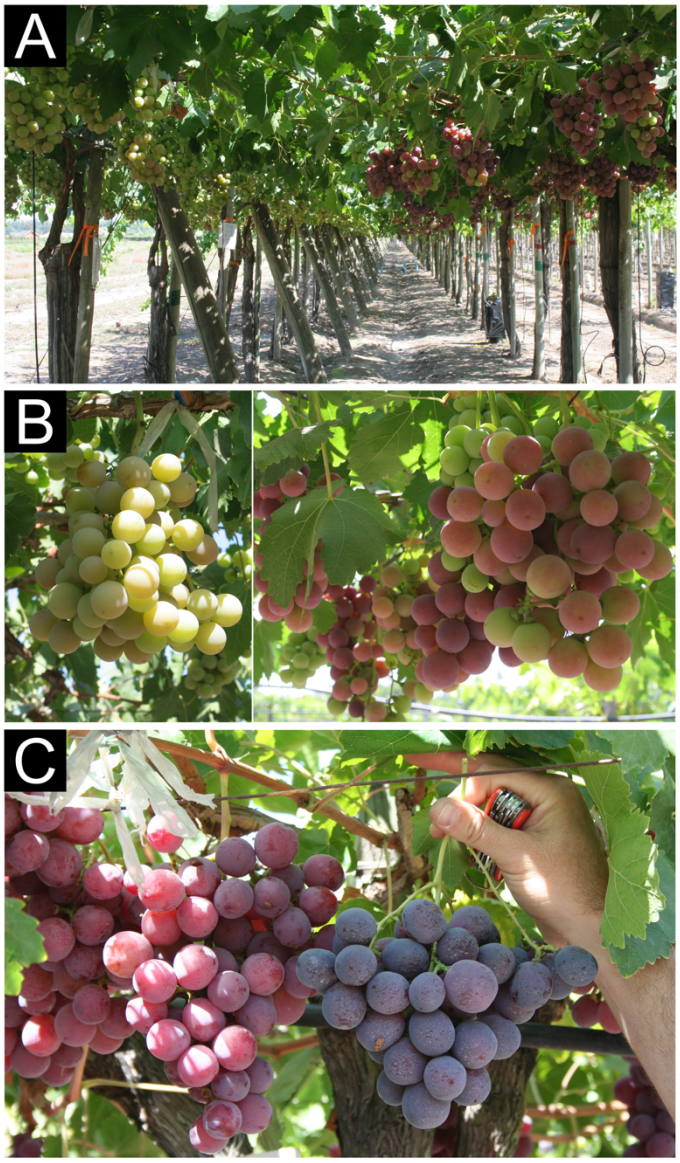


**FIGURE 1: Pigmentation differences at field of the color somatic variants under study.** **(A-B)** Cultivar (cv.) ‘Chimenti Globe’ (CG) and cv. ‘Red Globe’ (RG) at the onset of

ripening/veraison (EL-35) and **(C)** at a late ripening stage (EL-38)**.** Clusters of CG plants are shown at the left side of each photograph in all cases. Plants from both cultivars used in this study are situated immediately adjacent to each other in the same field.

**Microscopy**

Oblique hand sections of ripening berries were cut with a scalpel blade and floated on a glycerol 50% droplet and mounted on slices. Samples were examined under spectral confocal optical microscope *Eclipse C2si*, Nikon Instruments Inc. (Minato-ku, Tokyo, Japan).

**Metabolite extractions and quantification analyses**

For metabolite analyses, berry skins from both seasons were used and processed independently (24 total samples per cultivar), except for the case of anthocyanin analysis, for which five out of six samples were considered for each cultivar (20 samples per cultivar). Primary metabolites such as Trehalose-6-Phosphate (T6P) together with glycolytic and tricarboxylic acid (TCA) cycle intermediates were extracted from 25 mg of frozen powder with chloroform/methanol solution, and measured by high-performance anion-exchange liquid chromatography coupled to tandem mass spectrometry (LC-MS/MS) as described by (John E. Lunn et al., 2006). Amino acids were extracted and analyzed by HPLC as described by (Martínez-Lüscher et al., 2014). For sugars and organic acids, an aliquot of 150-200 mg of skin fine powder was extracted sequentially with ethanol 80% and 50%, dried in a SpeedVac and re-dissolved in 1 ml of sterile ultrapure water. Hexose content (glucose and fructose) was measured enzymatically with an automated micro-plate reader (Elx800UV, Biotek Instruments Inc., Winooski, VT, USA) according to (L. Gomez, Bancel, Rubio, & Vercambre, 2007). Tartaric acid content was measured by using the colorimetric method based on ammonium vanadate reactions (Pereira et al., 2006). Malic acid content was determined using an enzyme-coupled spectrophotometric method that measures the change in absorbance at 340 nm from the reduction of $NAD^+$ to NADH (Pereira et al., 2006).

Anthocyanins were extracted from 300 mg freeze-dried ground powder from skin of cv. ‘RG’ and ‘CG’ using 1 ml methanol containing 0.1% HCl (v/v). Extracts were filtered across 0.45 µm polypropylene syringe filter (Pall Gelman Corp., Ann Harbor, MI, USA) for high

153 performance liquid chromatography (HPLC) analysis. Each individual anthocyanin was
154 analyzed as described in (Dai et al., 2013). For anthocyanin quantification was integrated peak
155 area at 520 nm and using Malvidin 3-glucoside as standard (Extrasynthèse, Lyon, France).
156
157 **RNA extraction**
158 Total RNA were isolated from berry skins according to the procedure of (Reid, Olsson,
159 Schlosser, Peng, & Lund, 2006), using a CTAB-spermidine extraction buffer. This material was
160 used for transcriptome sequencing by RNA-seq technology and validation of data by
161 quantitative real-time RT-PCR (qRT-PCR). For RNA sequencing, berry skins from 2013 season
162 were used and pooled in 3 samples per cultivar (cv. 'CG' and 'RG') and stage (veraison and
163 ripening), reaching a total number of 12 samples to be deep sequenced. Each pool was generated
164 by mixing 2 individual RNA extractions (1 µg each one) and then mixing them to obtain a
165 concentration of 2 µg per pool (TABLE S1). Total RNA was sent to Macrogen (Macrogen Inc.
166 Seoul, Korea) after ethanol precipitation (0.1 volume of 3 M Sodium Acetate pH 7-8 and 2
167 volumes of 100% ethanol).
168
169 **RNA Sequencing and Read Mapping**
170 Ten micrograms of total RNA were fragmented, converted to cDNA, and amplified by
171 PCR to Illumina ® TruSeqTM RNA Sample Preparation Kit (Illumina, Inc., USA). Pair-end
172 100bp sequence reads were generated using the Illumina Genome Analyzer II (Illumina) and
173 Illumina HiSeq 2000 (Illumina) at Macrogen Inc. according to the manufacturer's
174 recommendations. Trimmomatic (Bolger, Lohse, & Usadel, 2014) was used to trim and clip
175 reads prior to mapping, removing the adapter sequences as well as the low-quality sequences
176 from the ends of the reads. All the distinct clean reads were aligned to the Grape Genome
177 Database hosted at CRIBI V2 (http://genomes.cribi.unipd.it/grape/) (Vitulo et al., 2014).
178 Uniquely mapped reads were counted by HITSAT2 software (Kim, Langmead, & Salzberg,
179 2015) and featureCounts in the Rsubread package (Liao, Smyth, & Shi, 2013).
180
181 **Analysis of differentially expressed genes (DEGs)**
182 DESeq2 was used for determining differentially expressed genes (DEGs) using a false

discovery rate (*FDR*) threshold of 0.05 and an absolute value $\log_2$ ratio ≥ 1 (Love, Huber, & Anders, 2014). MultiExperiment Viewer (MeV) was used for gene clustering analysis that was performed by the k-means method with Euclidean distance. MeV also was used for graphical representation of DEGs in a heatmap using Fold Change ≥ 1 (Howe, Sinha, Schlauch, & Quackenbush, 2011). Additionally, we performed a new DESeq2 analysis with the same parameters described previously but removing the filter from the Fold Change; the DEGs obtained with this method were annotated using Mercator web tool and then loaded into MapMan software (Lohse et al., 2014; Usadel et al., 2009).

**Validation of RNA-seq data by quantitative real-time RT-PCR (qRT-PCR)**

Two micrograms (ug) of total RNA were treated with TURBO DNA-freeTM DNase (Ambion®) and subsequently reverse transcribed with random hexamer primers and SuperScript II RT (InvitrogenTM Co., Carlsbad, CA, USA) as in (Dauelsberg et al., 2011). Relative transcript quantification of differentially expressed genes (DEGs) was performed by real-time RT-PCR (qRT-PCR) using the BRILLIANT II SYBR® GREEN QPCR Master Mix and the Mx3000P qPCR system (Stratagene, Agilent Technologies Inc., Santa Clara, CA, USA) according to the manufacturer's instructions. Expression levels of all evaluated genes were calculated from six biological replicates, relative to *Vvi60SRP* housekeeping control gene. We used the $2^{-\Delta\Delta Ct}$ method for the statistical analysis (Schefe, Lehmann, Buschmann, Unger, & Funke-Kaiser, 2006). Primers are listed in Supplementary (TABLE S2).

**Statistical data analyses**

Data were analyzed with multivariate analysis methods using the R statistics environment (R Core Team, 2010). In order to evaluate alterations in metabolite levels during stages of grapevine development, principal component analysis (PCA) was performed on mean-centered and scaled data using the ade4 package in R (Dray & Dufour, 2007). Differences between developmental stages and seasons were analyzed by a two-way ANOVA followed with a Tukey multiple comparison post-hoc test at $P < 0.05$, for example, in the case of PCA analysis, component 1. For differences between cultivars were analyzed using unpaired T-test, for example in the case of PCA analysis, component 2 and qRT-PCR analysis. GraphPad Prism version 6.00 for Windows (GraphPad Software, La Jolla California USA) was used for graphics

representation and analysis. For RNA-seq analysis, Trimmomatic (Bolger et al., 2014), HISAT2 (Kim et al., 2015) and Rsubread package (Liao et al., 2013) were used with default parameters. DEGs analysis were performed with DEseq2 using *FDR* with a threshold of 0.05 and absolute value $\log_2$ ratio ≥ 1 (Love et al., 2014). (MeV) was used for cluster analysis by the k-means method with Pearson's correlation distance and graphical representation of DEGs with a heatmap using FC ≥ 1 (Howe et al., 2011).

## RESULTS

### Characterization of cv. 'Red Globe' and its color somatic variant cv. 'Chimenti Globe'.

#### *Microscopy study*

Grape berry skin is composed of several cell layers: the epidermal cells comprising only a single layer (L1-derived) and the large underlying subepidermal cells (L2-derived) that also compromise the flesh. We observed in cv. 'Chimenti Globe' that anthocyanins only accumulated in the outermost single layer of the Epidermis (Ep) and not in the subEpidermis (subEp) (FIGURE 2A-B-C). A clear accumulation of anthocyanins was observed within the vacuoles of the epidermal cells, in Anthocyanin Vacuolar Inclusions (AVIs) (FIGURE 2C). This observation was similar to the previously characterized cv. 'Malian' (a bud sport of cv. 'Cabernet Sauvignon'; Walker et al., 2006) and cv. 'Pinot Gris' (a periclinal chimera of cv. 'Pinot Noir'; Vezzulli et al., 2012). In contrast, cv. 'Red Globe' showed colored cells in the Ep layer (FIGURE 2E), with diffuse edge, and some specific AVIs inside some subEp cells that form part of the skin (FIGURE 2D).

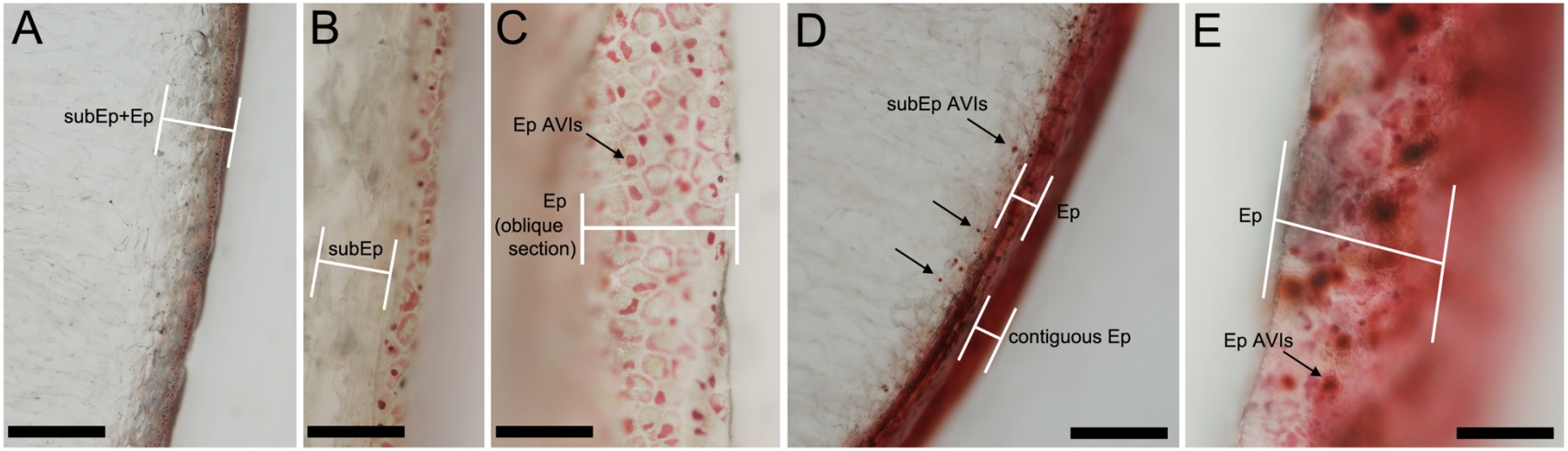


**FIGURE 2: Differential accumulation of anthocyanins in epidermal and subepidermal cell layers of CG and RG**. Light microscopy sections showing cells from the epidermis (Ep; L1 ontology) and subepidermis (subEp; L2 ontology) in cv. 'Chimenti Globe' **(A-C)** and cv. 'Red Globe' **(D-E)**. Anthocyanin vacuolar inclusions (AVIs) are depicted with arrows. Oblique angle hand sections permitted observe contiguous cells from the epidermis as in Walker et al. (2006). In both cultivars the mesocarp/flesh (L2 ontology) is devoid of anthocyanins. Bar in A and D is 500 μm; B, C and E is 100 μm

***Primary metabolite profiling identifies several compounds affected in the skin of 'CG'.***

The composition of the main primary metabolites was assessed by different methods depending of each metabolite (described in Methodology). Quantifications were analyzed with Principal Component Analysis (PCA) to obtain a comprehensive view of main metabolites showing differences between both somatic variants in veraison and ripening. The first two principal components ($PC_1$ and $PC_2$) explained about 64% of the total variance and allowed to discriminate developmental stages between CG and RG (FIGURE 3A). $PC_1$ (43,75%) was inferred to capture predominantly variation according to developmental stage and also to the effect of season but the latter exclusively for the ripening stage samples (no variation was observed for season at the veraison stage). Metabolites contributing to these differences were related to phenylpropanoid metabolism such as shikimate, UDP-glucose and phenylalanine but in addition the molecular regulator trehalose-6-phosphate (T6P) and TCA cycle intermediates such as citrate, isocitrate and several amino acids also contributed to differentiate veraison from ripening (FIGURE 3B and FIGURE S1). $PC_2$ variation (20,26%) was associated to cultivar type, but this discrimination was much more evident for the ripening stage samples. These results are explained in changes observed in metabolites related with biosynthesis of sucrose: glyceraldehyde 3-phosphate, fructose 6-phosphate, glucose 6-phosphate, fructose 1,6-biophosphate, glucose 1,6-biophosphate, glycerol 3-phosphate, fructose, glucose and phosphoenolpyruvate; and also, with anthocyanin compounds (FIGURE 3B and FIGURE S2).

*Anthocyanin profiles in berry.*

We analyzed anthocyanin levels present in berry skins of cv. 'RG' and its somatic variant 'CG' at the same developmental stages and seasons described previously. During the veraison stage, 'CG' showed trace amounts of some anthocyanin types (Table S3). At ripening, we observed the most significant differences in total anthocyanin abundances between cv. 'CG' and 'RG', with RG containing more than seven times higher amount (FIGURE 4A).

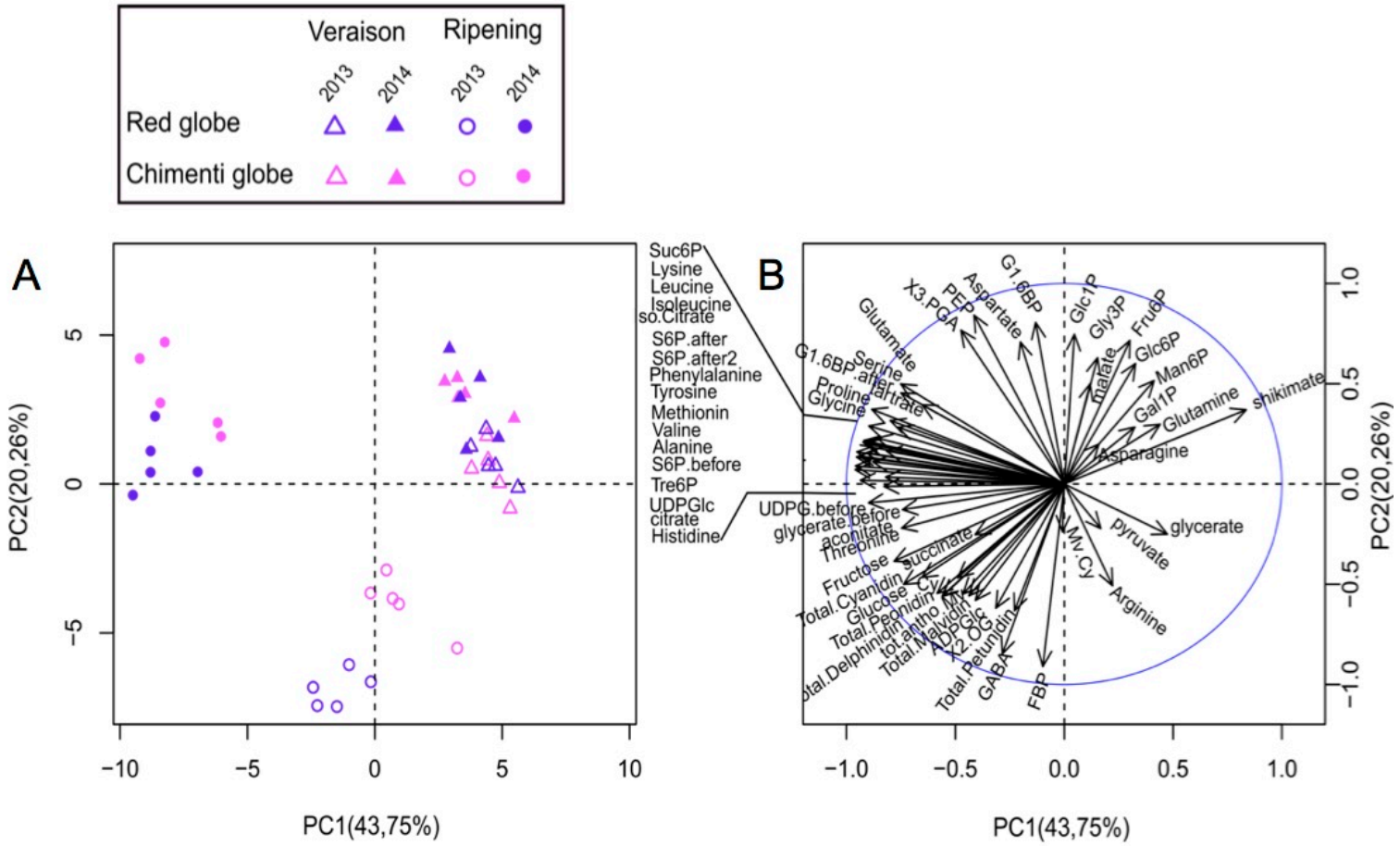


**FIGURE 3: Differential metabolomes in berries of color somatic variants influenced by developmental stage and vintage.** (A) Principal component analysis (PCA) of primary metabolites present in berry skins of RG and CG, discriminating by cultivar depending on the developmental stage. The variance explained by season (2013/2014) is implied at both stages but is more evident at the ripening stage. (B) Loading plots of metabolites analyzed for the first two components (PC1 and PC2). Main metabolites that explained PC1 correspond to those close to the ordinate axis such as tre6P, UDPGlc, methionine, phenylalanine and shikimate; and for PC2 correspond to those close to the abscissa axis such as phosphorylate intermediates and anthocyanins.

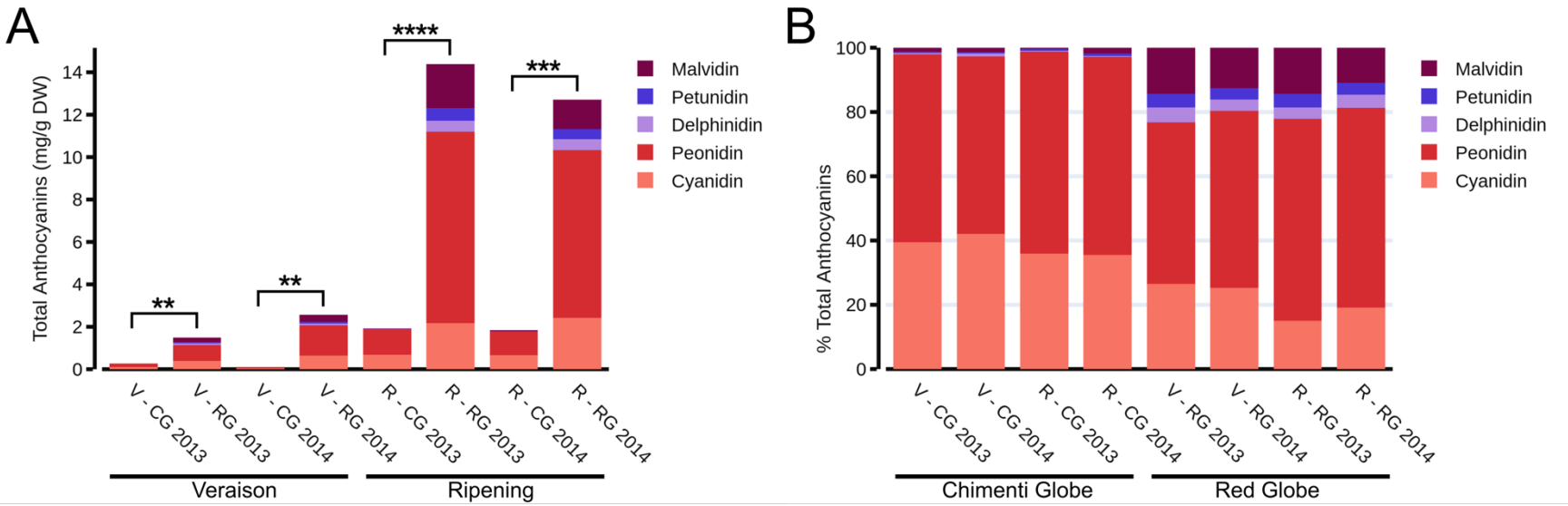


**FIGURE 4: The decreased anthocyanin content in cv. 'Chimenti Globe' is accentuated by the insufficiency in accumulating tri-hydroxylated derivatives.** (A) Content of total anthocyanins (mg $g^{-1}$ DW, all derivatives) in both somatic variants at veraison and ripening stages in 2013 and 2014 seasons. Asterisks indicate statistical significance as the result of an unpaired T-test. **, $P < 0.0081$; ***, $P = 0.0001$; ****, $P < 0.0001$.). (B) Relative abundance of each anthocyanin type for each sample. Di-hydroxylated derivatives found were cyanidin 3-glucoside, cyanidin 3-(*p*-coumaryl)-glucoside, peonidin-3-glucoside and peonidin-3-(*p*-coumaryl)-glucoside. Tri-hydroxylated derivatives found were delphinidin 3-glucoside, delphinidin 3-(acetyl)-glucoside, petunidin 3-glucoside and malvidin-3-glucoside. Values in (A) and (B) represent the mean of five biological replicates. Anthocyanin derivative content for each replicate can be found in Supplementary Table S3). DW: Dry Weight.

Detailed analysis of anthocyanin derivatives revealed that 'CG' mainly contains di-hydroxylated types, namely peonidin (in the form of peonidin 3-glucoside and peonidin 3-(*p*-coumaryl)-glucoside) and cyanidin (in the form of cyanidin 3-glucoside and cyanidin 3-(*p*-coumaryl)-glucoside), which confer more reddish tones (FIGURE 4B) compared to tri-hydroxylated forms. Tri-hydroxylated anthocyanins (the most commonly and abundantly found in black-skinned *V. vinifera* cultivars and that confer purplish and bluish colors), were present in very small amounts or even non-detectable in cv. 'CG', while they were found increasing towards ripening in cv. 'RG'. The proportion of total tri-hydroxylated derivatives with respect to that of di-hydroxylated forms was maintained relatively constant between veraison and ripening (between 20-35% of the total amount of anthocyanins), being Malvidin the most abundant of all three (TABLE S3).

## Genome-wide characterization of cv. 'Chimenti Globe' and 'Red Globe' transcriptomes.

### *RNA-Seq data mapping to the grapevine genome and category enrichment analysis.*

We originally hypothesized that the genes responsible for changes in berry skin color in cv. 'CG' should be differentially altered in expression when compared to cv. 'RG'. We performed mRNA-Seq profiling using twelve RNA samples corresponding to three independent pools of biological replicates for 'CG' and 'RG' for each developmental stage in the 2013 season (TABLE S1). From a total range of ~4.8 – 8.1 million sequencing raw read pairs, from each pool sample, only ~4.5 – 7.6 million read pairs corresponded to both kept reads that passed the quality analysis, representing a 93% of the total read pairs (TABLE S4). Approximately ~3.3 – 5.1 million reads aligned uniquely to the annotated transcriptome, while ~0.5 – 1.5 million reads aligned 0 times and ~0.7 – 1.2 million reads aligned multiple times (72%, 11-20% and 15-17% of the total reads after quality analysis, respectively) (TABLE S5). Only the reads that aligned uniquely and where mapped to the genome were further considered in the analysis (TABLE S5, S6).

To explore the differences between both color somatic variants, all clean reads were aligned to the grape genome database V2 (Vitulo et al., 2014) and then a comparative transcriptomic analysis was performed to screen for differentially expressed genes (DEGs) using

DEseq2 package (Love et al., 2014). The first inspection of the complete RNA-seq dataset showed that the major differences between both somatic variants are observed at ripening (FIGURE 5). The PC1, accounting for approximately 50% of the total variance, was able to discriminate 'CV' and 'RG' only at ripening while the PC2 accounted for differences mostly attributable to 'RG' at ripening compared to the three other samples (with the exception one replicate in CG ripening).

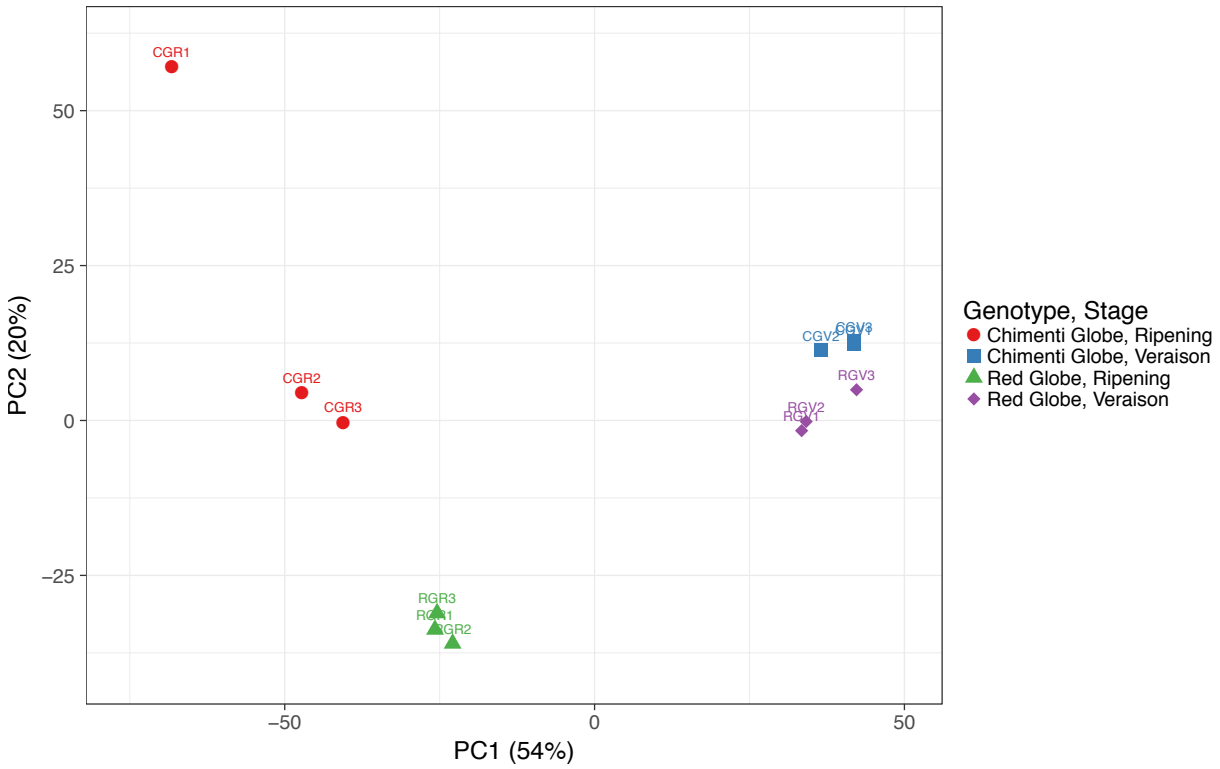


**FIGURE 5: PCA of transcriptomics data.** X and Y axis show principal component 1 and principal component 2 that explain 54% and 20% of the total variance, respectively. Original FPKM values are ln(x + 1)-transformed (NAs removed). No scaling was applied to individual genes and SVD with imputation was used to calculate principal components. N = 12 data points.

A total of 438 genes showed differential expression (log2FC>1 and p adjusted value<0.05) in at least one stage. We performed a Gene Ontology (GO) enrichment analysis to enlighten functional categories represented in the 438 DEGs (Supplemental Dataset 1), by using the Mercator web tool and then loaded into MapMan software version 3.5.1R2 (Lohse et al.,

2014; Usadel et al., 2009). Three major types of secondary metabolic pathways were differentially expressed between cultivars at veraison and ripening: terpenoids and the phenylpropanoid-related lignin/lignans and flavonoids (FIGURE S3). Additional categories found enriched were those related to enzymes families (e.g. cytochrome P450, UDP-glycosyltransferases, glutathione-S-transferases, glucosidases, o-methyltransferases, peroxidases and beta 1,3 glucan hydrolases, FIGURE S4), and those related to biotic stresses (FIGURE S5) including genes involved in the synthesis of stress-related hormones, pathogenesis related (PR) proteins and transcription factors, among others.

***The cultivar 'Chimenti Globe' exhibits an altered expression of the entire flavonoid pathway compared to cv. 'Red Globe'.***

From the 438 DEGs, a total of 109 genes were differentially expressed at both veraison and ripening stages. These were grouped in 6 clusters according to a hierarchical clustering of their expression profiles (FIGURE 6). From the 109 DEGs, many were related to flavonoid metabolism. Cluster A consisted in only one gene: a *glutathione-S-transferase* collinear with GST4 (VIT_204s0079g00710) that is involved in anthocyanin transport in grapes. Cluster B (23 genes) and cluster C (31 genes), where genes are down-regulated in cv. 'CG' at both developmental stages, contained many flavonoid/anthocyanin-related genes such as GST13 (VIT_207s0104g01800), GST4 (VIT_204s0079g00690), *flavonoid 3,5-hydroxylases* (F3'5'-H, VIT_206s0009g02805 – 2810 – 2830 – 2840 – 2846 – 2860 – 2873 – 2880 – 2970 – 2920 – 3010), *anthoMATEs (*AM1, VIT_216s0050g00900 and AM2, VIT_216s0050g00910*),* *flavanone 3-hydroxylase* (F3-H, VIT_204s0023g03370)*, anthocyanin membrane protein 1 (*ANM1, VIT_208s0007g03560*), anthocyanin acyltransferase (*3AT, VIT_203s0017g00870) *chalcone synthase* (CHS, VIT_205s0136g00260), anthocyanin-o-methyltranferases (AOMT1, VIT_201s0010g03510 and AOMT2, VIT_201s0010g03490) and *UDP-glucose:flavonoid 3-O-glucosyltransferase* (UFGT, VIT_216s0039g02230). These clusters also included the genes *vacuolar invertase 1* (GIN1, VIT_216s0022g00670) involved in sugar transport, *cellulose synthase (*CSLA02, VIT_206s0061g01230*)* and an uncharacterized *cytochrome b5* (CYTB5, VIT_218s0001g09400) (FIGURE 6). Another interesting gene repressed in cv. 'CG' in both developmental stages encodes a *homeobox-leucine zipper* (HD-Zip) transcription factor (VIT_216s0100g00670) homologue to *anthocyaninless 2,* a homeobox gene involved in

anthocyanin distribution and root development in Arabidopsis (Kubo, Peeters, Aarts, Pereira, & Koornneef, 1999) (FIGURE 6). Cluster E (34 genes) encompassed genes that were induced at both developmental stages in cv. 'CG', some of which may be related to phenylpropanoid metabolism, such as *cytochrome p450* (CYP71E1, VIT_201s0137g00540), *ABC transporter family protein* (VIT_214s0060g00720) and a *catechol-O-methyltransferases* (VIT_215s0048g02480-2490). The transcription factor *MYB24* (VIT_214s0066g01090) and a *sesquiterpene synthase* (TPS10, VIT_218s0001g04780) were also listed in this group. Cluster D (11 genes) and Cluster F (9 genes) combined genes with contrasting expressions at veraison and ripening. Genes falling in these categories included three (VIT_210s0042g00840, VIT_210s0042g00880 and VIT_210s0042g00920) and *ABC transporter G member 15* (VIT_209s0002g03560) that were induced at ripening but repressed in veraison (FIGURE 6).

We performed a less stringent analysis excluding the Fold Change filtering step to search for additional pathways altered by color somatic variation. Within transcription factors, we found that *MYBA1* (VIT_202s0033g00410), *MYBA8* (VIT_202s0033g00380), *MYB30B* (VIT_214s0108g00830), *MYB141* (VIT_214s0108g01080) and *MYB147* (VIT_217s0000g09080) were repressed at veraison in cv. 'CG', while the stilbene regulator *MYB15* (VIT_205s0049g01020), *MYB24* (VIT_214s0066g01090) and *MYB162* (VIT_219s0090g00590) were induced at this stage. The truncated and non-functional *MYBA3* gene (VIT_202s0033g00450, collinear with *MYBA1* and *MYBA2*), and *MYB24* were also induced at ripening. In contrast to what was observed at veraison, *MYB30B* was induced during ripening in cv. 'CG'. Furthermore, the flavonoid regulator *MYBPA1* (VIT_215s0046g00170) and *MYB145* (VIT_219s0014g03820) were repressed during the ripening stage in cv. 'CG'. Additional TF genes were differentially expressed in ripening cv. 'CG' berries, such as bHLH 145-like gene (VIT_218s0001g07210) and an uncharacterized WD repeat-containing protein C16727 isoform 1 (VIT_208s0007g00730), both being induced (Supplemental Dataset 2).

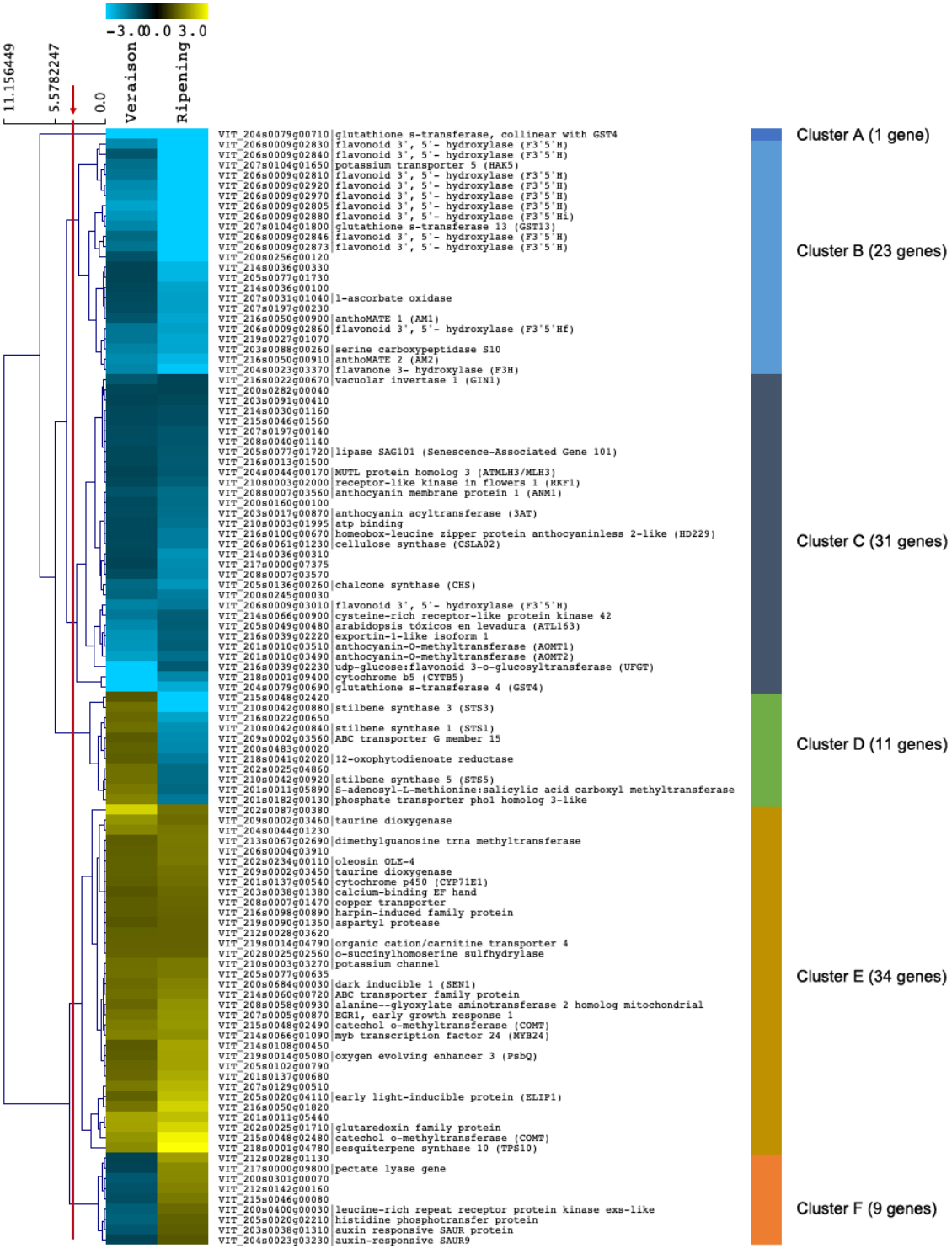


391

**FIGURE 6 (previous page): Differentially expressed genes (DEGs) associated to somatic color variation at both veraison and ripening as surveyed by RNA-seq.** Heatmap of 109 DEGs in CG compared to RG, where differential expression is defined by logFC>=1 of the CG/RG ratio and FDR<=0.05. Hierarchical clustering shows the presence of six major clusters outlined on the right panel (these were defined by cutting the dendrogram at the site shown by the red line). 12X.v1 (CRIBIv2 annotation) gene IDs were included for those genes with either an annotation or those previously characterized in grape with relevant functions to our study.

***Genes related to 'Primary metabolism'.***

Inspection of the less stringent list of DEGs allowed to identify several genes related to primary metabolism between cv. 'CG' and cv. 'RG'. At veraison, we identified genes related to sucrose and trehalose 6-phosphate biosynthesis and also to sugar transport, pathways that have been related in *Arabidopsis thaliana* to a homeostatic mechanism of maintaining sucrose levels within a range that is appropriate for each cell type and developmental stage of the plant (Tre6P:sucrose ratio; Yadav et al., 2014). The bidirectional sugar transporters *VviSWEET1* (VIT_218s0001g15330), *VviSWEET10* (VIT_217s0000g00830) and *VviSWEET15* (VIT_201s0146g00260), three hexose transporters (VIT_205s0020g03140, VIT_211s0149g00050 and VIT_214s0006g02720) and two genes encoding a fructose-bisphosphate aldolase (VIT_203s0038g00670 and VIT_204s0023g03010) were induced in cv. 'CG' in the veraison stage. At ripening, we observed genes related to sucrose and trehalose biosynthesis and sugar transportation such as *VviSWEET11* (VIT_207s0104g01340, induced in cv. 'CG'), two genes encoding a sucrose-phosphate synthase (VIT_218s0075g00330 and VIT_218s0089g00490, induced and repressed at ripening, respectively), a sucrose transporter and sucrose synthase 1 (VIT_201s0026g01960 and VIT_207s0005g00750) both being repressed. A fructose-1,6-bisphosphatase (VIT_208s0007g01570) and two genes putatively encoding a fructose-bisphosphate aldolase (VIT_204s0023g03010 and VIT_203s0038g00670) were induced. Finally, four genes putatively encoding a trehalose-phosphate synthase (VIT_206s0009g01650, VIT_217s0000g08010, VIT_203s0063g01510 and VIT_212s0028g01670) were induced in cv. 'CG' during ripening (Supplemental Dataset 3).

***Genes from other secondary metabolic pathways.***

Other genes found in the less-strict list were related to other metabolic pathways such as isoprenoid biosynthesis: two isoprene synthase genes up-regulated in cv. 'CG' at veraison (VIT_212s0134g00020, VIT_212s0134g00030) and ripening (VIT_212s0134g00030); and the carotenoid pathway: a probable carotenoid cleavage dioxygenase 4 gene down-regulated in cv. 'CG' during veraison (VIT_202s0087g00930). Amongst DEGs in cv. 'CG', the terpenoid biosynthesis pathway genes TPS35 (VIT_212s0134g00030) and TPS10 (VIT_218s0001g04780) were up-regulated both at veraison and ripening.

**Validation of the RNA-seq gene expression profiles.**

Twelve DEGs were selected for qRT-PCR validation (FIGURE 7). From clusters of down-regulated genes (clusters A, B and C) nine genes were selected: nine isoforms of *F3'5'-H*, *CYTB5*, *UFGT*, *AOMT1-2*, *AM1-2*, *GST13*, *F3H* and *CHS*. Seven of these genes (*F3'5'-H*, *CYTB5*, *UFGT, AOMT1-2, GST13, F3-H* and *CHS*) showed significant differences between cv. 'CG' and cv. 'RG' at veraison and ripening, fully supporting the RNA-seq results, while *AM1-2* only showed differences at the ripening stage (FIGURE 7).

**FIGURE 7 (next page): Real-time quantitative PCR (qRT-PCR) validation of selected DEGs in berry skins of CG and RG.** Samples were collected at veraison and ripening stages in 2013. Genes were selected based in their role or position in the repression, induction or combined repression/induction clusters. Gene expression in berries is shown relative to *SRP60* (VIT_205s0077g02060) housekeeping gene expression. Values represent the mean of six biological replicates, and bars represent the standard error of mean. These were derived from one qPCR run with duplicate PCR reactions on each of the biological replicates. Gene expressions were normalized together for both developmental stages. Asterisks indicate statistical significance as the result of unpaired T-test between both somatic variants, independently taken at each developmental stage (*, $P < 0.0465$; **, $P < 0.0053$; ***, $P < 0.0009$; ****, $P < 0.0001$). FW, Fresh Weight.

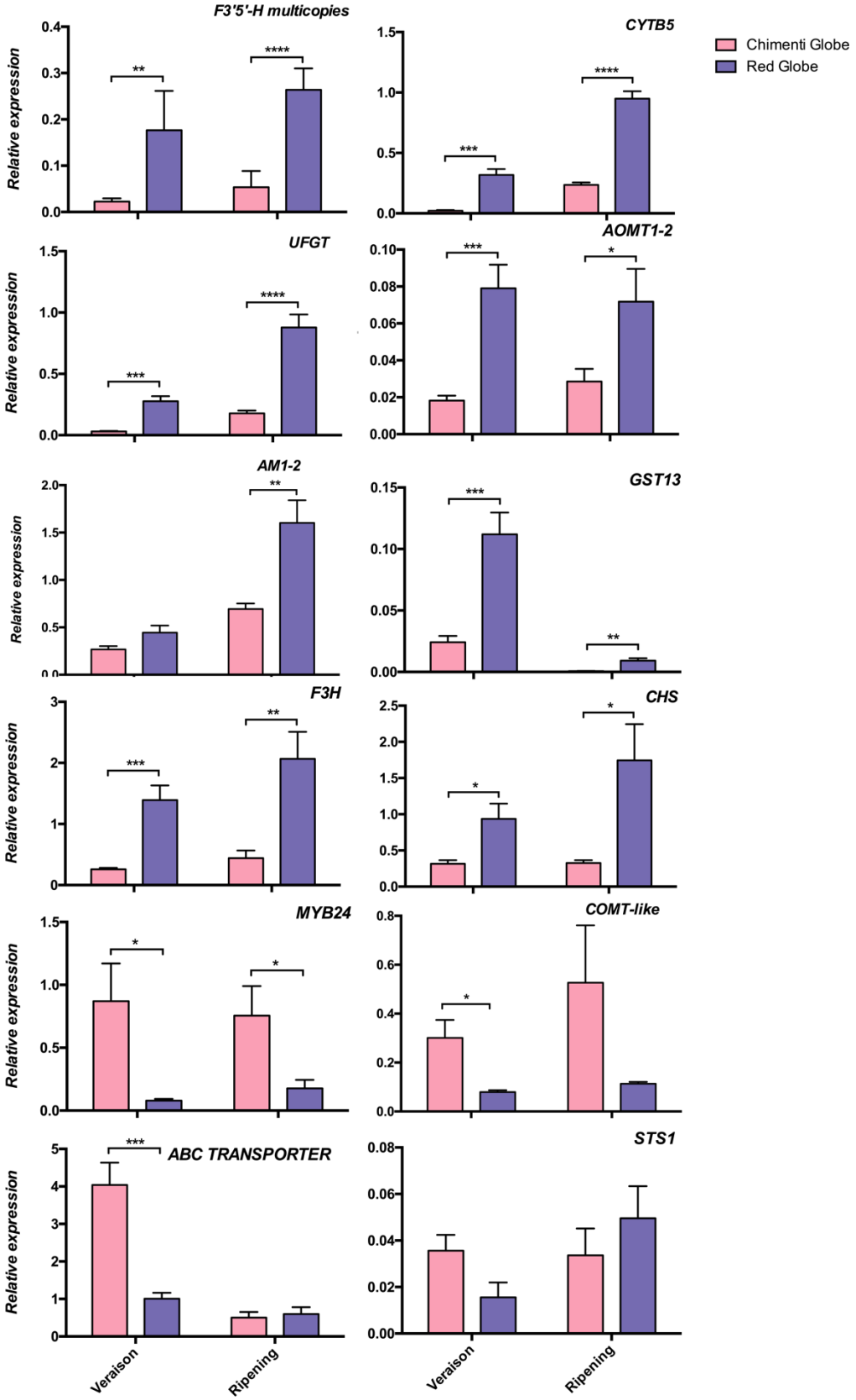

To gain more insight in gene expression of the nine isoforms of *F3'5'-H* we were able to design specific primers for six of them. In general, we observed significant differences in each isoform (i.e. induction in cv. 'RG' compared to cv. 'CG') at both stages (FIGURE S6B). We confirmed this observation by inspecting the specifically-assigned reads in the RNA-seq analysis (TABLE S7). From the Cluster of induced genes (Cluster E), three were further selected, validating *MYB24*'s significant induction in both veraison and ripening stages, while an *ABC transporter family protein* (VIT_214s0060g00720) and two *COMT-like* genes (designed primers recognized both VIT_215s0048g02480 and VIT_215s0048g02490) were induced in cv. 'CG' only at veraison (FIGURE 6). The *STS1* gene, that codified a Stilbene synthase was selected from clusters D, exhibiting a higher expression at ripening and a lower one at veraison in cv. 'CG' compared to cv. 'RG', but without significant differences.

We observed that within the list of genes belonging to the repression cluster on the heatmap generated (FIGURE 6) there were 11 copies of the gene *F3'5'-H* not induced in cv. 'CG': VIT_206s0009g02805, VIT_206s0009g02810, VIT_206s0009g02840, VIT_206s0009g02860, VIT_206s0009g02873, VIT_206s0009g02880, VIT_206s0009g02920, VIT_206s0009g02970 and VIT_206s0009g03010. These genes were located closely in the same region of chromosome 6 (FIGURE S6A). This corresponded to a segment of the chromosome that span from approximately 15,660 to 16,060 MB.

**Exploration of the MYBA color locus identifies MYBA1 as the only gene responsible for the skin color differences.**

In order to try to elucidate the genetic origin of the 'Chimenti Globe' phenotype, we checked the presence of MYBA1 white and red alleles in cv. 'CG' and cv. 'RG' using the same set of primers used in (Shimazaki et al., 2011), while also studied *MYBA1* expression levels by qPCR. We observed the presence of white and red alleles of *MYBA1* in all cv. 'CG' and cv. 'RG' samples tested (FIGURE 8), demonstrating that both cultivars are heterozygous for this gene, at least in the L2 cell layer. These results were validated with molecular marker analysis (TABLE S8), which in addition revealed a homozygous null allele configuration of MYBA2, in both L1 and L2 cell layers, in the two somatic variants. We further confirmed the null allele of MYBA2 in >99% samples (both cultivars) by inspecting all the reads matching the G/T positions related to MYBA2 mutation (i.e. variant calling analysis; TABLE S9). As MYBA2 is

non-functional in both cultivars, only the differences in *MYBA1* expression could account for the skin pigmentation differences of 'Chimenti Globe'. We tested *MYBA1* expression by qRT-PCR, observing that it was down-regulated at veraison (RNA-seq $log_2$FC -0,947) and ripening (confirmed only by qRT-PCR) in cv. 'CG' (FIGURE 8).

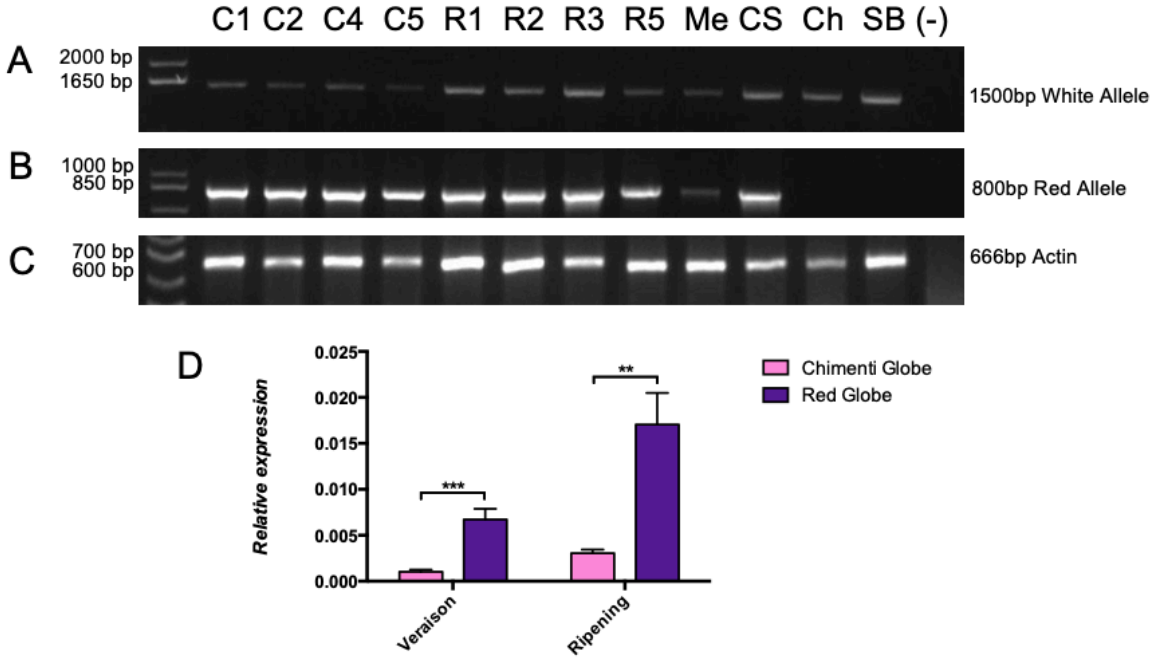


**FIGURE 8: Heterozygous *VviMYBA1* gene allelic configuration in both somatic variants and reduced *MYBA1* expression in cv. 'Chimenti Globe' compared to cv. 'Red Globe'.** (A-B) PCR identification of the (A) non-functional white allele and (B) functional red allele in cv. 'Chimenti Globe' (C1,2,3), cv. 'Red Globe' (R1,2,3), and other cultivars used as controls (cv. 'Merlot' -Me, cv. 'Cabernet Sauvignon' -CS, cv. 'Chardonnay' -Ch and cv. 'Sauvignon Blanc' -SB); (C) *ACTIN* gene amplification was used as an internal PCR control check for gDNA integrity. Numbers on the left side of each electrophoresis gel photograph indicate the band size according to the DNA marker ladder, while numbers on the right show the exact size of the white and red alleles according to (Shimazaki, Fujita, Kobayashi, & Suzuki, 2011). (D) qRT-PCR analysis of *VviMYBA1* in berry skins. Relative gene expression calculation as the mean of six biological replicates, with error bars representing the standard error of the mean. Asterisks indicate the result of unpaired T-test. **, $P = 0.0023$; ***, $P = 0.0007$.

## DISCUSSION

### Anthocyanin accumulation in the berry skin of cv. 'Chimenti Globe' is diminished in correlation to the repression of both *MYBA1* and the flavonoid/anthocyanin pathways.

Grape somatic variants have been well described in the literature and specifically those affecting skin pigmentation have become a source of new commercial genotypes (Azuma, 2018; Pelsy, 2010; Torregrosa et al., 2011; Vezzulli et al., 2012; Walker et al., 2006; Carbonell-Bejerano et al., 2017). In this work, we studied cv. 'Chimenti Globe' ('CG') that was originated as a somatic variation of cv. 'Red Globe' ('RG'). Microscopic analysis showed in ripe berries that cv. 'CG' had a particular pattern of anthocyanin accumulation, exclusive to the epidermis. In contrast, 'RG' also presented pigmentation in the sub-epidermis. This pattern was similarly described in cv. 'Malian' (Walker et al., 2006) and cv. 'Pinot Gris' (Vezzulli et al., 2012). The microscopy analysis allowed to suggest initially that cv. 'CG' was a periclinal chimera with only the L1 cell layer capable of producing anthocyanins. However, the molecular marker analysis showed that 'CG' was heterozygous for the functional *MYBA1* allele in the L2. Under this configuration, MYBA1 is still active and transcriptionally regulates the accumulation of anthocyanins in vacuoles (Ford, Boss, & Hoj, 1998). In the case of pink-skinned cultivars of oriental origin, Shimazaki et al. (2011) reported a 33bp insertion in the second intron of *VviMYBA1* as a consequence of low expression levels of *VviMYBA1*. Thus, it would be necessary to sequence *MYBA1*'s genomic region in both L1 and L2 derived tissues and see if there is any change that may account for *MYBA1* lower expression in 'CG'.

The lower *VviMYBA1* expression, together with the particular pattern of anthocyanin accumulation in cv. 'CG' observed by microscopy i.e. absence of anthocyanin vacuolar inclusions in subepidermal cells, allows to suggest anthocyanin transport as a possible process

526 being largely affected and responsible for diminished anthocyanin accumulation. In plant cells,
527 anthocyanins are synthesized in the cytoplasmatic face of the endoplasmic reticulum (Winkel-
528 Shirley, 2001; Winkel, 2004) and then are transported to the vacuole for storage. Three different
529 mechanisms have been described for flavonoid transport: membrane transporters, vesicle
530 trafficking and glutathione S-transferase (GST)- mediated transport (Zhao, 2015). In grapevine,
531 orthologs of TT12 have been identified, an Arabidopsis gene encoding a MATE protein required
532 for anthocyanin and proanthocyanidin accumulation in the vacuole (Marinova et al., 2007). In
533 addition, AM1 and AM3 transport acylated anthocyanins in the presence of Mg ATP (C. Gomez
534 et al., 2009); and *VviABCC1* transports malvidin 3-O-glucoside into vacuoles (Francisco et al.,
535 2013). The glutathione-S-transferases *VviGST1*, *VviGST3* and *VviGST4*, expressed in grape
536 fruits, have the ability to bind different flavonoid ligands (Pérez-Díaz, Madrid-Espinoza,
537 Salinas-Cornejo, González-Villanueva, & Ruiz-Lara, 2016). From the 109 differentially
538 expressed genes from our study, we observed several genes related to anthocyanin vacuolar
539 transportation being repressed in cv. 'CG': *GST* and two *anthoMATE* (AM1 and AM2) genes.
540 Interestingly, *VviGST4 and VviAM2* are specifically highly expressed at berry maturity (Sun et
541 al., 2016). Other genes down-regulated in cv. 'CG' were *ANM1*, encoding a putative
542 anthocyanin membrane protein 1, and *3AT* related with anthocyanin acylation, a process known
543 to improve anthocyanin intensity and color stabilization (Yonekura-Sakakibara, Nakayama,
544 Yamazaki, & Saito, 2008). All these genes are directly regulated by MYBA1 and in less
545 intensity by its homologues MYBA6 and MYBA7 (Matus et al., 2017)
546
547

**Metabolic changes during veraison and ripening stages in cv. 'Red Globe' and cv. 'Chimenti Globe'.**

Berry ripening is an active process that involves regulation of global gene expression (Fasoli et al., 2012) and changes in the accumulation of primary and secondary metabolites (Boss, Davies, & Robinson, 1996; Conde et al., 2007). Primary metabolites and in particular sugars are indeed elicitors of anthocyanin synthesis, reason why we decided to analyze them in this study. Metabolic comparison between the two somatic variants showed that the developmental stage was the primary discriminant parameter, despite the use of different cultivars. This observation is concordant with previous published studies (D.-L. Guo et al., 2016; Massonnet et al., 2017; D. C. J. Wong, Lopez Gutierrez, Dimopoulos, Gambetta, & Castellarin, 2016; Wu et al., 2014) in which, despite the use of different cultivars, the importance of developmental stages appeared to overrule cultivar origin. T6P seems a main influential metabolite (as seen in PC1, FIGURE 3A). T6P is a sugar phosphate considered as a metabolic signaling molecule in plants that regulates developmental growth (John Edward Lunn, Delorge, Figueroa, Van Dijck, & Stitt, 2014) and was demonstrated to be involved in sugar signaling in *Arabidopsis thaliana* (John E. Lunn et al., 2006). In *Vitis vinifera* there is no clear evidence of control of T6P during berry development, although several transcriptomic studies have shown that orthologue genes encoding T6P synthase, T6P synthase/phosphatase and SnRK1 (Sucrose-non-fermentative Related Kinase 1, i.e. another sugar signaling pathway component) are tightly regulated during berry development (Deluc et al., 2007; Gambetta, Matthews, Shaghasi, McElrone, & Castellarin, 2010). Although no significant differences were observed at the level of quantification of T6P, the analysis obtained from the RNA-seq analysis data (DEG analysis

570 without Fold Change filter) showed the down-regulation of four genes encoding trehalose -
571 phosphate synthase in cv. 'CG' during ripening).

572 Due to the fact that T6P modulates sugar signaling, we searched for DEGs between cv.
573 'RG' and cv. 'CG' related with sugar, fructose, glucose and sucrose biosynthesis in our RNA-
574 seq analysis. We identified three genes at veraison, *VviSWEET1* (VIT_218s0001g15330),
575 *VviSWEET10* (VIT_217s0000g00830) and *VviSWEET15* (VIT_201s0146g00260) and in
576 ripening *VviSWEET11* (VIT_207s0104g01340), as induced in cv. 'CG'. These constitute a
577 protein family of sugar uniporters involved in sugar export (Chen et al., 2010; Chong et al.,
578 2014; W.-J. Guo et al., 2014). Indeed, it has been described that several SWEET proteins in *V.*
579 *vinifera* increase from veraison onwards in cv. 'Syrah' and cv. 'Muscatel Ottonel' (Chong et al.,
580 2014). Despite these genes are less expressed in green berries, *VviSWEET1* is the mainly
581 expressed in young and adult leaves; *VviSWEET10* and *VViSWEET11* in flowers; *VviSWEET10*,
582 *VviSWEET11* and *VviSWEET15* in berries after veraison (Chong et al., 2014).

583 We found other genes related directly with sucrose biosynthesis induced in cv. 'CG': two
584 fructose-bisphosphate aldolases (VIT_203s0038g00670 and VIT_204s0023g03010) were
585 induced during veraison and ripening stage. This enzyme catalyzes the conversion of
586 glyceraldehyde 3-phosphate (PGAL) to fructose 1,6- bisphosphate (F1,6-BP). Concordantly, we
587 also found that these metabolites were decreased in cv. 'CG' during ripening stage in 2013, and
588 in fact was one of the metabolites that explained the differences observed in cultivars (PC2 ,
589 FIGURE 3A). A similar pattern was observed with fructose-1,6-bisphosphatase
590 (VIT_208s0007g01570), induced in cv. 'CG'. This enzyme catalyzes the conversion of F1,6-
591 BP to fructose 6-phosphate (F6-P), which was found decreased in cv. 'CG' at ripening. The
592 sucrose-phosphate synthases encoded by VIT_218s0075g00330 and VIT_218s0089g00490

593 catalyze the conversion of uridine diphosphate-glucose (UDP-glucose) to glucose-fructose-
594 phosphate (GF-P), leading to the last step of sucrose biosynthesis (Ruan, 2014).

595 Taking all these observations together, it is possible to suggest an alteration in cv. 'CG'
596 occurring at the level of sugar export and in sucrose biosynthesis. This process could be related
597 to the anthocyanin biosynthesis pathway in cv. 'CG' as anthocyanin accumulation in plants can
598 be induced by sugar (Das, Shin, Choi, & Park, 2012). Specifically in grapevines, fructose,
599 glucose and sucrose induce anthocyanin accumulation (Dai et al., 2013; Larronde et al., 1998;
600 Zheng et al., 2009).

601 Among primary metabolites occurring in the intersection with secondary metabolism, we
602 found shikimate as significant. This is an intermediary of the shimikate pathway that mediates
603 the carbon flow from carbohydrate metabolism to phenylpropanoid and aromatic compound
604 biosynthesis (Maeda & Dudareva, 2012; Zhang et al., 2012). This strongly suggest the
605 importance of this metabolite in species such as grapevine, in which the berry consumes
606 phenylalanine for the biosynthesis of flavonoid compounds such as anthocyanins.

607 Anthocyanins explained major differences in the PC analysis of metabolites. We observed
608 that only traces of malvidin, petunidin and delphinidin were detected in cv. 'CG', indicating a
609 block in the tri-hydroxylated branch of the anthocyanin biosynthesis pathway, an observation
610 latter confirmed by the RNA-seq analysis. Accordingly, an increase in F3'5'-H activity has been
611 previously reported to explain higher concentration of tri-hydroxylated anthocyanins in
612 Cabernet Sauvignon and Shiraz, pinpointing F3'5'-Hs as key molecular players driving the
613 phenylpropanoid metabolic flux towards bluish anthocyanin production (Degu et al., 2014).

614

615

**Transcriptomic changes during veraison and ripening in cv. 'CG' and cv. 'RG'**

In our study, besides metabolic studies, the skin transcriptomes of both somatic variants were analyzed using Illumina Hiseq2000. We report that several genes related to flavonoid pathway, grouped in three main clusters, were differentially expressed in cv. 'CG' compared to cv. 'RG'. Among these, we identified eleven *F3'5'-H* isoforms repressed in cv. 'CG', consistent with the depletion of delphinidin-type anthocyanins. The adjacent location of each one of these copies in a single cluster within chromosome 6 (FIGURE S6A; Castellarin et al., 2006; Falginella et al., 2010) allows to suggest a common regulation for all of them, presumably by MYBA1 and other TFs. *CYTB5* was down-regulated in cv. 'CG' at both stages. *CYBT5* has been previously involved in F3'5'-H activity modulation in Petunia flowers, catalyzing the transfer of electrons to their prosthetic heme group (de Vetten et al., 1999). In 2006, (Jochen Bogs, Ebadi, McDavid, & Robinson, 2006) demonstrated that a putative *CYBT5* from grapevine cv. 'Shiraz' modulated both F3'5'-H and F3'-H activities even though the exact mechanism remains to be deciphered. This is of interest because this suggests a possible link regarding the drastic down-regulation of eleven gene copies of F3'5'-H.

Three *Stilbene synthase* genes (*STS1, STS3* and *STS5*), involved in resveratrol biosynthesis (Dubrovina & Kiselev, 2017; Kiselev, Aleynova, Grigorchuk, & Dubrovina, 2016) were induced in cv. 'CG' at veraison and down-regulated during ripening stage. MYB15 is involved in the transcriptional regulation of stilbene synthases in grapevine (Holl et al., 2013) and was also induced in cv. 'CG'. This suggests a possible compensation point in flavonoid metabolism: CHS utilizes the same substrates as STS but, is responsible for flavonoid-type compound formation. Chalcone synthase (*CHS*) was indeed down-regulated in cv. 'CG', in correlation with less total anthocyanins. Thus, STS could act as an escape valve to reflux the

639 exceeded carbon after the decrease in CHS activity. Taken together, this would suggest a
640 multilevel alteration of the flavonoid pathway, and not only of its anthocyanin tri-hydroxylated
641 branch in cv. 'CG'.
642
643 **The berry color locus shows similar allelic configurations in both somatic variants.**
644 White skinned grape cultivars that do not produce anthocyanins contain a *MYBA1* null
645 allele in homozygosity, in which the presence of the retrotransposon *Gret1* in the
646 promoter/5'UTR region interrupts the normal transcription (Kobayashi et al., 2004). Pigmented
647 cultivars possess at least one functional 'red berry' allele either without *Gret1* or with the
648 excised retrotransposon (This et al., 2007). We observed the presence of white and red alleles
649 of *MYBA1* in all cv. 'CG' and cv. 'RG' samples tested, thus, it seems that the allelic
650 configuration of *MYBA1* is not responsible for the phenotype differences. Despite this, the
651 down-regulation of flavonoid and anthocyanin structural genes in cv. 'CG' is only possibly
652 related to MYBA1, as MYBA2 appears non-functional in all meristematic cell layers and
653 cultivars. The significant differences of *MYBA1* expression between both cultivars at veraison
654 and ripening should be the responsible of the changes in anthocyanin abundance (including the
655 changes in di/tri-hydroxylated anthocyanin profiles). The expression of *MYBA1* in 'Chimenti'
656 is decreased by a different process not identified here.

## AUTHOR CONTRIBUTIONS

EG, PAJ, SD and JTM designed experiments. CS performed material sampling, RNA extraction, for deep sequencing and qRT-PCR, gathered all the results and wrote the manuscript. TM and CM conducted the bioinformatics analyses and data mining. JL and RF carried out the LC-MS/MS metabolic analysis. GH and CR assisted in hexose, anthocyanin and organic acids quantifications. LM assisted in RNA extraction and material sampling collection. RA and DC performed molecular marker analysis. JTM reanalyzed RNA-seq data, produced PCA plots, edited figures and together with FMN, EG, PAJ and SD revised the manuscript.

## ACKNOWLEDGMENTS

We thank to CONICYT scholarship doctorate 2012 Nº 21120432, Operational Expenses Scolarship of CONICYT Nº 21120432, Millennium Nucleus of Plant Systems and Synthetic Biology NC130030, FONDECYT 1150220 and CHIMENTI S.A. This work was also supported by Grant PGC2018-099449-A-I00 and by the Ramón y Cajal program grant RYC-2017-23645, both awarded to J.T.M. from the Ministerio de Ciencia, Innovación y Universidades (MCIU, Spain), Agencia Estatal de Investigación (AEI, Spain), and Fondo Europeo de Desarrollo Regional (FEDER, European Union).

674 **REFERENCES**

675

676 Azuma, A. (2018). Genetic and Environmental Impacts on the Biosynthesis of Anthocyanins
677 in Grapes. *The Horticulture Journal*. https://doi.org/10.2503/hortj.OKD-IR02
678 Azuma, A., Kobayashi, S., Mitani, N., Shiraishi, M., Yamada, M., Ueno, T., … Koshita, Y.
679 (2008). Genomic and genetic analysis of Myb-related genes that regulate anthocyanin
680 biosynthesis in grape berry skin. *Theoretical and Applied Genetics*, *117*(6), 1009–1019.
681 https://doi.org/10.1007/s00122-008-0840-1
682 Bogs, J, Jaffe, F. W., Takos, A. M., Walker, A. R., & Robinson, S. P. (2007). The grapevine
683 transcription factor VvMYBPA1 regulates proanthocyanidin synthesis during fruit
684 development. *Plant Physiol*, *143*. https://doi.org/10.1104/pp.106.093203
685 Bogs, Jochen, Ebadi, A., McDavid, D., & Robinson, S. P. (2006). Identification of the
686 flavonoid hydroxylases from grapevine and their regulation during fruit development.
687 *Plant Physiology*, *140*(1), 279–291. https://doi.org/10.1104/pp.105.073262
688 Bolger, A. M., Lohse, M., & Usadel, B. (2014). Trimmomatic: A flexible trimmer for
689 Illumina sequence data. *Bioinformatics*, *30*(15), 2114–2120.
690 https://doi.org/10.1093/bioinformatics/btu170
691 Boss, P. K., Davies, C., & Robinson, S. P. (1996). Anthocyanin composition and anthocyanin
692 pathway gene expression in grapevine sports differing in berry skin colour. *Australian*
693 *Journal of Grape and Wine Research*, *2*(3), 163–170. https://doi.org/10.1111/j.1755-
694 0238.1996.tb00104.x
695 Carbonell-Bejerano, P., Diago, M.-P., Martínez-Abaigar, J., Martínez-Zapater, J. M.,
696 Tardáguila, J., & Núñez-Olivera, E. (2014). Solar ultraviolet radiation is necessary to
697 enhance grapevine fruit ripening transcriptional and phenolic responses. *BMC Plant*
698 *Biology*, *14*(1), 183. https://doi.org/10.1186/1471-2229-14-183
699 Carbonell-Bejerano P, Royo C, Torres-Pérez R, Grimplet J, Fernandez L, Franco-Zorrilla
700 JM, et al. Catastrophic unbalanced genome rearrangements cause somatic loss of berry
701 color in grapevine. Plant Physiol 2017;175:pp.00715.2017. doi:10.1104/pp.17.00715.
702 Cardoso, S., Lau, W., Dias, J. E., Fevereiro, P., & Maniatis, N. (2012). A Candidate-Gene
703 Association Study for Berry Colour and Anthocyanin Content in Vitis vinifera L. *PLoS*
704 *ONE*, *7*(9). https://doi.org/10.1371/journal.pone.0046021

705 Carrier, G., Le Cunff, L., Dereeper, A., Legrand, D., Sabot, F., Bouchez, O., … This, P.
706 (2012). Transposable elements are a major cause of somatic polymorphism in vitis
707 vinifera L. *PLoS ONE*, *7*(3), 1–10. https://doi.org/10.1371/journal.pone.0032973
708 Castellarin, S. D., Di Gaspero, G., Marconi, R., Nonis, A., Peterlunger, E., Paillard, S., …
709 Testolin, R. (2006). Colour variation in red grapevines (Vitis vinifera L.): genomic
710 organisation, expression of flavonoid 3'-hydroxylase, flavonoid 3',5'-hydroxylase
711 genes and related metabolite profiling of red cyanidin-/blue delphinidin-based
712 anthocyanins in berry skin. *BMC Genomics*, *7*, 12. https://doi.org/10.1186/1471-2164-
713 7-12
714 Chen, L. Q., Hou, B. H., Lalonde, S., Takanaga, H., Hartung, M. L., Qu, X. Q., … Frommer,
715 W. B. (2010). Sugar transporters for intercellular exchange and nutrition of pathogens.
716 *Nature*, *468*(7323), 527–532. https://doi.org/10.1038/nature09606
717 Chong, J., Piron, M. C., Meyer, S., Merdinoglu, D., Bertsch, C., & Mestre, P. (2014). The
718 SWEET family of sugar transporters in grapevine: VvSWEET4 is involved in the
719 interaction with Botrytis cinerea. *Journal of Experimental Botany*, *65*(22), 6589–6601.
720 https://doi.org/10.1093/jxb/eru375
721 Conde, C., Silva, P., Fontes, N., Dias, A. C. P., Tavares, R. M., Sousa, M. J., … Gerós, H.
722 (2007). Biochemical changes throughout grape berry development and fruit and wine
723 quality. *Food*, *1*, 1–22. https://doi.org/10.1093/jxb/ert395
724 COOMBE, B. G. (1995). Growth Stages of the Grapevine: Adoption of a system for
725 identifying grapevine growth stages. *Australian Journal of Grape and Wine Research*,
726 *1*(2), 104–110. https://doi.org/10.1111/j.1755-0238.1995.tb00086.x
727 Dai, Z. W., Meddar, M., Renaud, C., Merlin, I., Hilbert, G., Delrot, S., & Gomès, E. (2013).
728 Long-term in vitro culture of grape berries and its application to assess the effects of
729 sugar supply on anthocyanin accumulation. *Journal of Experimental Botany*, *65*(16),
730 4665–4677. https://doi.org/10.1093/jxb/ert489
731 Das, P. K., Shin, D. H., Choi, S., & Park, Y. (2012). *Sugar-Hormone Cross-Talk in*
732 *Anthocyanin Biosynthesis*. 501–507. https://doi.org/10.1007/s10059-012-0151-x
733 Dauelsberg, P., Matus, J. T., Poupin, M. J., Leiva-Ampuero, A., Godoy, F., Vega, A., &
734 Arce-Johnson, P. (2011). Effect of pollination and fertilization on the expression of
735 genes related to floral transition, hormone synthesis and berry development in

736 grapevine. *Journal of Plant Physiology*, *168*(14), 1667–1674.
737 https://doi.org/10.1016/j.jplph.2011.03.006
738 Davis, C., & Robinson, S. (1996). Sugar accumulation in grape berries. *Plant Physiol*, *111*(1
739 996), 275–283. https://doi.org/10.1007/bf02194096
740 de Vetten, N., ter Horst, J., van Schaik, H.-P., de Boer, A., Mol, J., & Koes, R. (1999). *A*
741 *cytochrome b 5 is required for full activity of flavonoid 3',5' -hydroxylase , a*
742 *cytochrome P450 involved in the formation of blue flower colors*. *96*(January), 778–
743 783.
744 Degu, A., Hochberg, U., Sikron, N., Venturini, L., Buson, G., Ghan, R., … Fait, A. (2014).
745 Metabolite and transcript profiling of berry skin during fruit development elucidates
746 differential regulation between Cabernet Sauvignon and Shiraz cultivars at branching
747 points in the polyphenol pathway. *BMC Plant Biology*, *14*(1), 1–20.
748 https://doi.org/10.1186/s12870-014-0188-4
749 Deluc, L. G., Grimplet, J., Wheatley, M. D., Tillett, R. L., Quilici, D. R., Osborne, C., …
750 Cramer, G. R. (2007). Transcriptomic and metabolite analyses of Cabernet Sauvignon
751 grape berry development. *BMC Genomics*, *8*, 429. https://doi.org/10.1186/1471-2164-
752 8-429
753 Dray, S., & Dufour, A.-B. (2007). The **ade4** Package: Implementing the Duality Diagram for
754 Ecologists. *Journal of Statistical Software*, *22*(4). https://doi.org/10.18637/jss.v022.i04
755 Dubrovina, A., & Kiselev, K. (2017). Regulation of stilbene biosynthesis in plants. *Planta*.
756 https://doi.org/10.1007/s00425-017-2730-8
757 Falginella, L., Castellarin, S. D., Testolin, R., Gambetta, G. A., Morgante, M., & Di Gaspero,
758 G. (2010). Expansion and subfunctionalisation of flavonoid 3',5'-hydroxylases in the
759 grapevine lineage. *BMC Genomics*, *11*(1), 562. https://doi.org/10.1186/1471-2164-11-
760 562
761 Fasoli, M., Dal Santo, S., Zenoni, S., Tornielli, G. B., Farina, L., Zamboni, a., … Pezzotti,
762 M. (2012). The Grapevine Expression Atlas Reveals a Deep Transcriptome Shift
763 Driving the Entire Plant into a Maturation Program. *The Plant Cell*, *24*(9), 3489–3505.
764 https://doi.org/10.1105/tpc.112.100230
765 Ford, C. M., Boss, P. K., & Hoj, P. B. (1998). Cloning and characterization of Vitis vinifera
766 UDP-glucose:flavonoid 3-O-glucosyltransferase, a homolog of the enzyme encoded by

767 the maize bronze-1 locus that may primarily serve to glucosylate anthocyanidins in vivo.
768 *Journal of Biological Chemistry*, *273*(15), 9224–9233.
769 https://doi.org/10.1074/jbc.273.15.9224
770 Fortes, A. M., Agudelo-Romero, P., Silva, M. S., Ali, K., Sousa, L., Maltese, F., … Pais, M.
771 S. (2011). Transcript and metabolite analysis in Trincadeira cultivar reveals novel
772 information regarding the dynamics of grape ripening. *BMC Plant Biology*, *11*(1), 149.
773 https://doi.org/10.1186/1471-2229-11-149
774 Fraige, K., González-Fernández, R., Carrilho, E., & Jorrín-Novo, J. V. (2015). Metabolite
775 and proteome changes during the ripening of Syrah and Cabernet Sauvignon grape
776 varieties cultured in a nontraditional wine region in Brazil. *Journal of Proteomics*, *113*,
777 206–225. https://doi.org/10.1016/j.jprot.2014.09.021
778 Francisco, R. M., Regalado, A., Ageorges, A., Burla, B. J., Bassin, B., Eisenach, C., … Nagy,
779 R. (2013). ABCC1, an ATP Binding Cassette Protein from Grape Berry, Transports
780 Anthocyanidin 3- *O* -Glucosides. *The Plant Cell*, *25*(5), 1840–1854.
781 https://doi.org/10.1105/tpc.112.102152
782 Gambetta, G. A., Matthews, M. A., Shaghasi, T. H., McElrone, A. J., & Castellarin, S. D.
783 (2010). Sugar and abscisic acid signaling orthologs are activated at the onset of ripening
784 in grape. *Planta*, *232*(1), 219–234. https://doi.org/10.1007/s00425-010-1165-2
785 Ghan, R., Petereit, J., Tillett, R. L., Schlauch, K. A., Toubiana, D., Fait, A., & Cramer, G. R.
786 (2017). The common transcriptional subnetworks of the grape berry skin in the late
787 stages of ripening. *BMC Plant Biology*, *17*(1), 94. https://doi.org/10.1186/s12870-017-
788 1043-1
789 Ghan, R., Van Sluyter, S. C., Hochberg, U., Degu, A., Hopper, D. W., Tillet, R. L., …
790 Cramer, G. R. (2015). Five omic technologies are concordant in differentiating the
791 biochemical characteristics of the berries of five grapevine (Vitis vinifera L.) cultivars.
792 *BMC Genomics*, *16*(1), 946. https://doi.org/10.1186/s12864-015-2115-y
793 Gomez, C., Terrier, N., Torregrosa, L., Vialet, S., Fournier-Level, A., Verriès, C., …
794 Ageorges, A. (2009). Grapevine MATE-Type Proteins Act as Vacuolar
795 H<sup>+</sup>-Dependent Acylated Anthocyanin Transporters. *Plant*
796 *Physiology*, *150*(1), 402 LP – 415. Retrieved from
797 http://www.plantphysiol.org/content/150/1/402.abstract

798 Gomez, L., Bancel, D., Rubio, E., & Vercambre, G. (2007). The microplate reader: an
799 efficient tool for the separate enzymatic analysis of sugars in plant tissues—validation
800 of a micro-method. *Journal of the Science of Food and Agriculture*, *87*(10), 1893–1905.
801 https://doi.org/10.1002/jsfa.2924
802 Guo, D.-L., Xi, F.-F., Yu, Y.-H., Zhang, X.-Y., Zhang, G.-H., & Zhong, G.-Y. (2016).
803 Comparative RNA-Seq profiling of berry development between table grape 'Kyoho'
804 and its early-ripening mutant 'Fengzao'. *BMC Genomics*, *17*(1), 795.
805 https://doi.org/10.1186/s12864-016-3051-1
806 Guo, W.-J., Nagy, R., Chen, H.-Y., Pfrunder, S., Yu, Y.-C., Santelia, D., … Martinoia, E.
807 (2014). SWEET17, a Facilitative Transporter, Mediates Fructose Transport across the
808 Tonoplast of Arabidopsis Roots and Leaves. *Plant Physiology*, *164*(2), 777–789.
809 https://doi.org/10.1104/pp.113.232751
810 He, F., Mu, L., Yan, G. L., Liang, N. N., Pan, Q. H., Wang, J., … Duan, C. Q. (2010).
811 Biosynthesis of anthocyanins and their regulation in colored grapes. *Molecules*, *15*(12),
812 9057–9091. https://doi.org/10.3390/molecules15129057
813 Hichri, I., Heppel, S. C., Pillet, J., Léon, C., Czemmel, S., Delrot, S., … Bogs, J. (2010). The
814 basic helix-loop-helix transcription factor MYC1 is involved in the regulation of the
815 flavonoid biosynthesis pathway in grapevine. *Molecular Plant*, *3*(3), 509–523.
816 https://doi.org/10.1093/mp/ssp118
817 Hocquigny, S., Pelsy, F., Dumas, V., Kindt, S., Heloir, M.-C., & Merdinoglu, D. (2004).
818 Diversification within grapevine cultivars goes through chimeric states. *Genome*, *47*(3),
819 579–589. https://doi.org/10.1139/g04-006
820 Holl, J., Vannozzi, A., Czemmel, S., D'Onofrio, C., Walker, A. R., Rausch, T., … Bogs, J.
821 (2013). The R2R3-MYB Transcription Factors MYB14 and MYB15 Regulate Stilbene
822 Biosynthesis in Vitis vinifera. *The Plant Cell*, *25*(10), 4135–4149.
823 https://doi.org/10.1105/tpc.113.117127
824 Howe, E. A., Sinha, R., Schlauch, D., & Quackenbush, J. (2011). *RNA-Seq analysis in MeV*.
825 *27*(22), 3209–3210. https://doi.org/10.1093/bioinformatics/btr490
826 Hugueney, P., Provenzano, S., Verries, C., Ferrandino, A., Meudec, E., Batelli, G., …
827 Ageorges, A. (2009). A Novel Cation-Dependent O-Methyltransferase Involved in
828 Anthocyanin Methylation in Grapevine. *Plant Physiology*, *150*(4), 2057–2070.

https://doi.org/10.1104/pp.109.140376

Kim, D., Langmead, B., & Salzberg, S. L. (2015). HISAT: a fast spliced aligner with low memory requirements. *Nature Methods*, *12*(4), 357–360. https://doi.org/10.1038/nmeth.3317

Kiselev, K. V, Aleynova, O. A., Grigorchuk, V. P., & Dubrovina, A. S. (2016). *Stilbene accumulation and expression of stilbene biosynthesis pathway genes in wild grapevine Vitis amurensis Rupr* . https://doi.org/10.1007/s00425-016-2598-z

Kobayashi, S., Goto-Yamamoto, N., & Hirochika, H. (2004). Retrotransposon-induced mutations in grape skin color. *Science (New York, N.Y.)*, *304*(5673), 982. https://doi.org/10.1126/science.1095011

Kubo, H., Peeters, A. J. M., Aarts, M. G. M., Pereira, A., & Koornneef, M. (1999). ANTHOCYANINLESS2, a homeobox gene affecting anthocyanin distribution and root development in arabidopsis. *Plant Cell*, *11*(7), 1217–1226. https://doi.org/10.1105/tpc.11.7.1217

Kuhn, N., Guan, L., Dai, Z. W., Wu, B. H., Lauvergeat, V., Gomès, E., … Delrot, S. (2014). Berry ripening: Recently heard through the grapevine. *Journal of Experimental Botany*, *65*(16), 4543–4559. https://doi.org/10.1093/jxb/ert395

Larronde, F., Krisa, S., Decendit, A., Chèze, C., Deffieux, G., & Mérillon, J. M. (1998). Regulation of polyphenol production in Vitis vinifera cell suspension cultures by sugars. *Plant Cell Reports*, *17*(12), 946–950. https://doi.org/10.1007/s002990050515

Li, Q., He, F., Zhu, B.-Q., Liu, B., Sun, R.-Z., Duan, C.-Q., … Wang, J. (2014). Comparison of distinct transcriptional expression patterns of flavonoid biosynthesis in Cabernet Sauvignon grapes from east and west China. *Plant Physiology and Biochemistry : PPB / Société Française de Physiologie Végétale*, *84*(17), 45–56. https://doi.org/10.1016/j.plaphy.2014.08.026

Liao, Y., Smyth, G. K., & Shi, W. (2013). The Subread aligner: Fast, accurate and scalable read mapping by seed-and-vote. *Nucleic Acids Research*, *41*(10). https://doi.org/10.1093/nar/gkt214

Lijavetzky, D., Carbonell-Bejerano, P., Grimplet, J., Bravo, G., Flores, P., Fenoll, J., … Martínez-Zapater, J. M. (2012). Berry flesh and skin ripening features in Vitis vinifera as assessed by transcriptional profiling. *PLoS ONE*, *7*(6).

https://doi.org/10.1371/journal.pone.0039547

Lijavetzky, D., Ruiz-García, L., Cabezas, J. A., De Andrés, M. T., Bravo, G., Ibáñez, A., … Martínez-Zapater, J. M. (2006). Molecular genetics of berry colour variation in table grape. *Molecular Genetics and Genomics*, *276*(5), 427–435. https://doi.org/10.1007/s00438-006-0149-1

Lohse, M., Nagel, A., Herter, T., May, P., Schroda, M., Zrenner, R., … Usadel, B. (2014). Mercator: A fast and simple web server for genome scale functional annotation of plant sequence data. *Plant, Cell and Environment*, *37*(5), 1250–1258. https://doi.org/10.1111/pce.12231

Love, M. I., Huber, W., & Anders, S. (2014). Moderated estimation of fold change and dispersion for RNA-seq data with DESeq2. *Genome Biology*, *15*(12), 550. https://doi.org/10.1186/s13059-014-0550-8

Lunn, John E., Feil, R., Hendriks, J. H. M., Gibon, Y., Morcuende, R., Osuna, D., … Stitt, M. (2006). Sugar-induced increases in trehalose 6-phosphate are correlated with redox activation of ADPglucose pyrophosphorylase and higher rates of starch synthesis in *Arabidopsis thaliana*. *Biochemical Journal*, *397*(1), 139–148. https://doi.org/10.1042/BJ20060083

Lunn, John Edward, Delorge, I., Figueroa, C. M., Van Dijck, P., & Stitt, M. (2014). Trehalose metabolism in plants. *Plant Journal*, *79*(4), 544–567. https://doi.org/10.1111/tpj.12509

Maeda, H., & Dudareva, N. (2012). The shikimate pathway and aromatic amino Acid biosynthesis in plants. *Annual Review of Plant Biology*, *63*, 73–105. https://doi.org/10.1146/annurev-arplant-042811-105439

Marinova, K., Pourcel, L., Weder, B., Schwarz, M., Barron, D., Routaboul, J., … Klein, M. (2007). *The Arabidopsis MATE Transporter TT12 Acts as a Vacuolar Flavonoid / H 1 -Antiporter Active in Proanthocyanidin-Accumulating Cells of the Seed Coat*. *19*(June), 2023–2038. https://doi.org/10.1105/tpc.106.046029

Martínez-Lüscher, J., Sánchez-Díaz, M., Delrot, S., Aguirreolea, J., Pascual, I., & Gomès, E. (2014). Ultraviolet-B Radiation and Water Deficit Interact to Alter Flavonol and Anthocyanin Profiles in Grapevine Berries through Transcriptomic Regulation. *Plant and Cell Physiology*, *55*(September 2014), 1925–1936. https://doi.org/10.1093/pcp/pcu121

Massonnet, M., Fasoli, M., Tornielli, G. B., Altieri, M., Sandri, M., Zuccolotto, P., … Pezzotti, M. (2017). Ripening Transcriptomic Program in Red and White Grapevine Varieties Correlates with Berry Skin Anthocyanin Accumulation. *Plant Physiology*, *174*(4), 2376–2396. https://doi.org/10.1104/pp.17.00311

Matus, J. T., Poupin, M. J., Cañón, P., Bordeu, E., Alcalde, J. A., & Arce-Johnson, P. (2010). Isolation of WDR and bHLH genes related to flavonoid synthesis in grapevine (Vitis vinifera L.). *Plant Molecular Biology*, *72*(6), 607–620. https://doi.org/10.1007/s11103-010-9597-4

Matus, José Tomás, Cavallini, E., Loyola, R., Höll, J., Finezzo, L., Dal Santo, S., … Arce-Johnson, P. (2017). A group of grapevine MYBA transcription factors located in chromosome 14 control anthocyanin synthesis in vegetative organs with different specificities compared with the berry color locus. *Plant Journal*, *91*(2), 220–236. https://doi.org/10.1111/tpj.13558

Negri, A. S., Prinsi, B., Failla, O., Scienza, A., & Espen, L. (2015). Proteomic and metabolic traits of grape exocarp to explain different anthocyanin concentrations of the cultivars. *Frontiers in Plant Science*, *6*(August), 603. https://doi.org/10.3389/fpls.2015.00603

Niu, N., Wu, B., Yang, P., & Li, S. (2013). Comparative analysis of the dynamic proteomic profiles in berry skin between red and white grapes (Vitis vinifera L.) during fruit coloration. *Scientia Horticulturae*, *164*, 238–248. https://doi.org/10.1016/j.scienta.2013.09.046

Palumbo, M. C., Zenoni, S., Fasoli, M., Massonnet, M., Farina, L., Castiglione, F., … Paci, P. (2014). Integrated Network Analysis Identifies Fight-Club Nodes as a Class of Hubs Encompassing Key Putative Switch Genes That Induce Major Transcriptome Reprogramming during Grapevine Development. *The Plant Cell Online*, *26*(12), 4617–4635. https://doi.org/10.1105/tpc.114.133710

Pelsy, F. (2010). Molecular and cellular mechanisms of diversity within grapevine varieties. *Heredity*, *104*(4), 331–340. https://doi.org/10.1038/hdy.2009.161

Pelsy, Frédérique, Dumas, V., Bévilacqua, L., Hocquigny, S., & Merdinoglu, D. (2015). Chromosome Replacement and Deletion Lead to Clonal Polymorphism of Berry Color in Grapevine. *PLOS Genetics*, *11*(4), e1005081. https://doi.org/10.1371/journal.pgen.1005081

Pereira, G. E., Gaudillere, J. P., Pieri, P., Hilbert, G., Maucourt, M., Deborde, C., … Rolin, D. (2006). Microclimate influence on mineral and metabolic profiles of grape berries. *Journal of Agricultural and Food Chemistry*, *54*(18), 6765–6775. https://doi.org/10.1021/jf061013k

Pérez-Díaz, R., Madrid-Espinoza, J., Salinas-Cornejo, J., González-Villanueva, E., & Ruiz-Lara, S. (2016). Differential Roles for VviGST1, VviGST3, and VviGST4 in Proanthocyanidin and Anthocyanin Transport in Vitis vinífera. *Frontiers in Plant Science*, *7*(August), 1166. https://doi.org/10.3389/fpls.2016.01166

Petrussa, E., Braidot, E., Zancani, M., Peresson, C., Bertolini, A., Patui, S., & Vianello, A. (2013). *Plant Flavonoids — Biosynthesis , Transport and Involvement in Stress Responses*. 14950–14973. https://doi.org/10.3390/ijms140714950

R Core Team. (2010). No Title. *Vienna: R Foundation for Statistical Computing.*

Reid, K. E., Olsson, N., Schlosser, J., Peng, F., & Lund, S. T. (2006). An optimized grapevine RNA isolation procedure and statistical determination of reference genes for real-time RT-PCR during berry development. *BMC Plant Biology*, *6*, 27. https://doi.org/10.1186/1471-2229-6-27

Ruan, Y.-L. (2014). Sucrose Metabolism: Gateway to Diverse Carbon Use and Sugar Signaling. *Annual Review of Plant Biology*, *65*(1), 33–67. https://doi.org/10.1146/annurev-arplant-050213-040251

Savoi, S., Wong, D. C. J., Arapitsas, P., Miculan, M., Bucchetti, B., Peterlunger, E., … Castellarin, S. D. (2016). Transcriptome and metabolite profiling reveals that prolonged drought modulates the phenylpropanoid and terpenoid pathway in white grapes (Vitis vinifera L.). *BMC Plant Biology*, *16*(1), 67. https://doi.org/10.1186/s12870-016-0760-1

Schefe, J. H., Lehmann, K. E., Buschmann, I. R., Unger, T., & Funke-Kaiser, H. (2006). Quantitative real-time RT-PCR data analysis: Current concepts and the novel "gene expression's C T difference" formula. *Journal of Molecular Medicine*, *84*(11), 901–910. https://doi.org/10.1007/s00109-006-0097-6

Serrano, A., Espinoza, C., Armijo, G., Inostroza-Blancheteau, C., Poblete, E., Meyer-Regueiro, C., … Arce-Johnson, P. (2017). Omics Approaches for Understanding Grapevine Berry Development: Regulatory Networks Associated with Endogenous Processes and Environmental Responses. *Frontiers in Plant Science*, *8*(September), 1–

15. https://doi.org/10.3389/fpls.2017.01486

Shimazaki, M., Fujita, K., Kobayashi, H., & Suzuki, S. (2011). Pink-colored grape berry is the result of short insertion in intron of color regulatory gene. *PLoS ONE*, *6*(6), 1–8. https://doi.org/10.1371/journal.pone.0021308

Sun, L., Fan, X., Zhang, Y., Jiang, J., Sun, H., & Liu, C. (2016). Transcriptome analysis of genes involved in anthocyanins biosynthesis and transport in berries of black and white spine grapes (Vitis davidii). *Hereditas*, *153*, 17. https://doi.org/10.1186/s41065-016-0021-1

Sweetman, C., Wong, D. C., Ford, C. M., & Drew, D. P. (2012). Transcriptome analysis at four developmental stages of grape berry (Vitis vinifera cv. Shiraz) provides insights into regulated and coordinated gene expression. *BMC Genomics*, *13*(1), 691. https://doi.org/10.1186/1471-2164-13-691

Teixeira, A., Eiras-Dias, J., Castellarin, S. D., & Gerós, H. (2013). Berry phenolics of grapevine under challenging environments. *International Journal of Molecular Sciences*, *14*(9), 18711–18739. https://doi.org/10.3390/ijms140918711

This, P., Lacombe, T., Cadle-Davidson, M., & Owens, C. L. (2007). Wine grape (Vitis vinifera L.) color associates with allelic variation in the domestication gene VvmybA1. *Theoretical and Applied Genetics*, *114*(4), 723–730. https://doi.org/10.1007/s00122-006-0472-2

Torregrosa, L., Fernandez, L., Bouquet, A., Boursiquot, J. M., Pelsy, F., & Martinez-Zapater, J. M. (2011). Origins and Consequences of Somatic Variation in Grapevine. *Genetics, Genomics, and Breeding of Grapes*, (May), 68–92. https://doi.org/doi:10.1201/b10948-4

Usadel, B., Poree, F., Nagel, A., Lohse, M., Czedik-Eysenberg, A., & Stitt, M. (2009). A guide to using MapMan to visualize and compare Omics data in plants: A case study in the crop species, Maize. *Plant, Cell and Environment*, *32*(9), 1211–1229. https://doi.org/10.1111/j.1365-3040.2009.01978.x

Vezzulli, S., Leonardelli, L., Malossini, U., Stefanini, M., Velasco, R., & Moser, C. (2012). Pinot blanc and Pinot gris arose as independent somatic mutations of Pinot noir. *Journal of Experimental Botany*, *63*(18), 6359–6369. https://doi.org/10.1093/jxb/ers290

Vitulo, N., Forcato, C., Carpinelli, E., Telatin, A., Campagna, D., D'Angelo, M., … Valle,

984 G. (2014). A deep survey of alternative splicing in grape reveals changes in the splicing
985 machinery related to tissue, stress condition and genotype. *BMC Plant Biology*, *14*(1),
986 99. https://doi.org/10.1186/1471-2229-14-99
987 Walker, A. R., Lee, E., Bogs, J., McDavid, D. A. J., Thomas, M. R., & Robinson, S. P. (2007).
988 White grapes arose through the mutation of two similar and adjacent regulatory genes.
989 *Plant Journal*, *49*(5), 772–785. https://doi.org/10.1111/j.1365-313X.2006.02997.x
990 Walker, A. R., Lee, E., & Robinson, S. P. (2006). Two new grape cultivars, bud sports of
991 Cabernet Sauvignon bearing pale-coloured berries, are the result of deletion of two
992 regulatory genes of the berry colour locus. *Plant Molecular Biology*, *62*(4–5), 623–635.
993 https://doi.org/10.1007/s11103-006-9043-9
994 Wang, H., Wang, W., Zhan, J., Yan, A., Sun, L., Zhang, G., … Xu, H. (2016). The
995 accumulation and localization of chalcone synthase in grapevine (Vitis vinifera L.). In
996 *Plant Physiology and Biochemistry*. https://doi.org/10.1016/j.plaphy.2016.04.042
997 Winkel-Shirley, B. (2001). Flavonoid Biosynthesis. A Colorful Model for Genetics,
998 Biochemistry, Cell Biology, and Biotechnology. *Plant Physiology*, *126*(2), 485 LP –
999 493. Retrieved from http://www.plantphysiol.org/content/126/2/485.abstract
1000 Winkel, B. S. J. (2004). Metabolic Channeling in Plants. *Annual Review of Plant Biology*,
1001 *55*(1), 85–107. https://doi.org/10.1146/annurev.arplant.55.031903.141714
1002 Wong, D. C. J., Lopez Gutierrez, R., Dimopoulos, N., Gambetta, G. A., & Castellarin, S. D.
1003 (2016). Combined physiological, transcriptome, and cis-regulatory element analyses
1004 indicate that key aspects of ripening, metabolism, and transcriptional program in grapes
1005 (Vitis vinifera L.) are differentially modulated accordingly to fruit size. *BMC Genomics*,
1006 *17*(1), 416. https://doi.org/10.1186/s12864-016-2660-z
1007 Wong, Darren C. J., & Matus, J. T. (2017). Constructing Integrated Networks for Identifying
1008 New Secondary Metabolic Pathway Regulators in Grapevine: Recent Applications and
1009 Future Opportunities. *Frontiers in Plant Science*, *8*(April), 1–8.
1010 https://doi.org/10.3389/fpls.2017.00505
1011 Wong, Darren Chern Jan, Schlechter, R., Vannozzi, A., Höll, J., Hmmam, I., Bogs, J., …
1012 Matus, J. T. (2016). A systems-oriented analysis of the grapevine R2R3-MYB
1013 transcription factor family uncovers new insights into the regulation of stilbene
1014 accumulation. *DNA Research*, *23*(5), 451–466. https://doi.org/10.1093/dnares/dsw028

1015 Wu, B. H., Cao, Y. G., Guan, L., Xin, H. P., Li, J. H., & Li, S. H. (2014). Genome-wide
1016 transcriptional profiles of the berry skin of two red grape cultivars (Vitis vinifera) in
1017 which anthocyanin synthesis is sunlight-dependent or - Independent. *PLoS ONE*, *9*(8).
1018 https://doi.org/10.1371/journal.pone.0105959
1019 Xie, H., Konate, M., Sai, N., Tesfamicael, K. G., Cavagnaro, T., Gilliham, M., … Lopez, C.
1020 M. R. (2017). Global DNA Methylation Patterns Can Play a Role in Defining Terroir in
1021 Grapevine (Vitis vinifera cv. Shiraz). *Frontiers in Plant Science*, *8*(October), 1–16.
1022 https://doi.org/10.3389/fpls.2017.01860
1023 Yadav, U. P., Ivakov, A., Feil, R., Duan, G. Y., Walther, D., Giavalisco, P., … Lunn, J. E.
1024 (2014). The sucrose-trehalose 6-phosphate (Tre6P) nexus: Specificity and mechanisms
1025 of sucrose signalling by. *Journal of Experimental Botany*, *65*(4), 1051–1068.
1026 https://doi.org/10.1093/jxb/ert457
1027 Yakushiji, H., Kobayashi, S., Goto-Yamamoto, N., Tae Jeong, S., Sueta, T., MI, N., &
1028 Azuma, A. (2006). A Skin Color Mutation of Grapevine, from Black-Skinned Pinot
1029 Noir to White-Skinned Pinot Blanc, Is Caused by Deletion of the Functional VvmybA1
1030 Allele. *Bioscience, Biotechnology, and Biochemistry*, *70*(6), 1506–1508.
1031 https://doi.org/10.1271/bbb.50647
1032 Yonekura-Sakakibara, K., Nakayama, T., Yamazaki, M., & Saito, K. (2008). Modification
1033 and Stabilization of Anthocyanins. In *Anthocyanins* (Vol. 2, pp. 169–190).
1034 https://doi.org/10.1007/978-0-387-77335-3_6
1035 Zarrouk, O., Vialet, S., Marlin, T., Chaves, M., Martinoia, E., & Nagy, R. (2013). *ABCC1 ,*
1036 *an ATP Binding Cassette Protein from Grape Berry , Transports Anthocyanidin 3- O -*
1037 *Glucosides*. *25*(May), 1840–1854. https://doi.org/10.1105/tpc.112.102152
1038 Zenoni, S., Ferrarini, A., Giacomelli, E., Xumerle, L., Fasoli, M., Malerba, G., …
1039 Delledonne, M. (2010). Characterization of transcriptional complexity during berry
1040 development in Vitis vinifera using RNA-Seq. *Plant Physiology*, *152*(4), 1787–1795.
1041 https://doi.org/10.1104/pp.109.149716
1042 Zenoni, Sara, Fasoli, M., Guzzo, F., Dal Santo, S., Amato, A., Anesi, A., … Tornielli, G. B.
1043 (2016). Disclosing the Molecular Basis of the Postharvest Life of Berry in Different
1044 Grapevine Genotypes. *Plant Physiology*, *172*(3), 1821–1843.
1045 https://doi.org/10.1104/pp.16.00865

1046 Zhang, Z. Z., Li, X. X., Chu, Y. N., Zhang, M. X., Wen, Y. Q., Duan, C. Q., & Pan, Q. H.
1047 (2012). Three types of ultraviolet irradiation differentially promote expression of
1048 shikimate pathway genes and production of anthocyanins in grape berries. *Plant*
1049 *Physiology and Biochemistry*, *57*, 74–83. https://doi.org/10.1016/j.plaphy.2012.05.005
1050 Zhao, J. (2015). Flavonoid transport mechanisms : how to go , and with whom. *Trends in*
1051 *Plant Science*, 1–10. https://doi.org/10.1016/j.tplants.2015.06.007
1052 Zheng, Y., Tian, L., Liu, H., Pan, Q., Zhan, J., & Huang, W. (2009). Sugars induce
1053 anthocyanin accumulation and flavanone 3-hydroxylase expression in grape berries.
1054 *Plant Growth Regulation*, *58*(3), 251–260.
1055